cmgh
CELLULAR AND MOLECULAR GASTROENTEROLOGY AND HEPATOLOGY

ORIGINAL RESEARCH

Activation of AMP-activated Protein Kinase by Metformin Inhibits Dedifferentiation of Platelet-derived Growth Factor-BB-induced Vascular Smooth Muscle Cells to Improve Arterial Remodeling in Cirrhotic Portal Hypertension

Guangbo Wu,* Qiang Fan,* Min Chen,* Guqing Luo, Zhenghao Wu, Jinbo Zhao, Jiayun Lin, Chihao Zhang, Hongjie Li, Xiaoliang Qi, Haizhong Huo, Lei Zheng, and Meng Luo

Department of General Surgery, Shanghai Ninth People's Hospital Affiliated to Shanghai Jiao Tong University School of Medicine, Shanghai, China

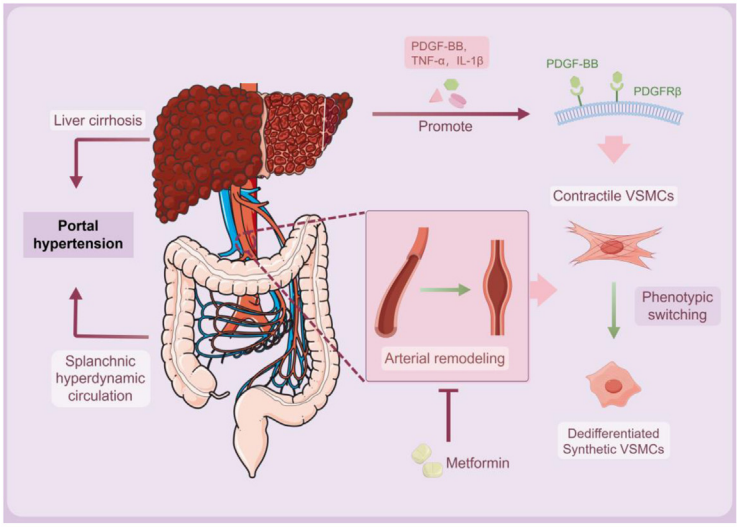

SUMMARY

Our study provides a meaningful contribution to the amelioration of splanchnic hyperdynamic circulation in cirrhotic rats with portal hypertension. We present the first insights into the potential mechanisms of arterial remodeling in liver cirrhosis from the perspective of vascular smooth muscle cells. By targeting AMP-activated protein kinase activation to hinder the dedifferentiation of contractile vascular smooth muscle cells, metformin exhibits promising improvements in arterial remodeling in cirrhotic rats. These findings not only deepen our understanding of arterial remodeling mechanisms in liver cirrhosis with portal hypertension but also inspire the development of targeted therapies aimed at reducing life-threatening vascular complications in cirrhotic patients.

BACKGROUND & AIMS: Portal hypertension (PHT) is the potentially deadly complication of liver cirrhosis. Intrahepatic vascular resistance and the splanchnic hyperdynamic circulation are 2 principal driving factors contributing to the maintenance and exacerbation of PHT. However, in the advanced stages of cirrhosis, the fibrotic process in the liver becomes irreversible, leading to persistent and intractable increases in intrahepatic vascular resistance. Arterial remodeling emerges as a crucial mechanism driving the hyperdynamic splanchnic circulation. Therefore, ameliorating the hyperdynamic splanchnic circulation has become an indispensable component of PHT therapeutic strategies.

METHODS: Liver cirrhosis with PHT was induced in the rats by common bile duct ligation (BDL). Based on the transcriptomic sequencing of the mesenteric arteries, we investigated the effects and mechanisms of metformin on the arterial remodeling at different stages of cirrhosis. We further validated potential molecular mechanisms through *in vitro* experiments using the A7r5 smooth muscle cell line and primary vascular smooth muscle cells (VSMCs).

RESULTS: Our findings revealed the beneficial effects of metformin on liver cirrhosis and PHT in rats following BDL for 4 and 6 weeks. Metformin was observed to ameliorate PHT and splanchnic hyperdynamic circulation in BDL rats, even in the advanced stages of liver cirrhosis. This effect was evidenced by reduced portal pressure and cardiac output, decreased superior mesenteric artery (SMA) flow, accompanied by improvements

in systemic vascular resistance and SMA resistance. Moreover, chronic inflammation in BDL rats was alleviated by metformin, which might inhibit the driving factors of angiogenesis and arterial remodeling. Notably, SMA dilation and arterial remodeling in BDL rats were potent alleviated following metformin treatment. Metformin ameliorated arterial remodeling in BDL rats by inhibiting the dedifferentiation of contractile VSMCs, resulting in the upregulation of contractile protein expressions such as alpha-smooth muscle actin (α-SMA) and smooth muscle 22α (SM22α). Platelet-derived growth factor-BB (PDGF-BB)/platelet-derived growth factor receptor beta (PDGFR-β) signaling exerted crucial roles in regulating the VSMCs cell phenotype. Activation of AMP-activated protein kinase (AMPK) by metformin blocked the downstream pathway of PDGF-BB/PDGFRβ. Furthermore, *in vitro* cell experiments, VSMCs were respectively treated with AMPK activator metformin or AMPK inhibitor Compound C. We revealed the molecular mechanism that metformin inhibited the phenotypic switching of A7r5 cells induced by PDGF-BB and primary VSMCs from BDL rats, which was mediated by activating AMPK to enhance the expression of contractile protein α-SMA. These findings suggest that AMPK can ameliorate the progression of arterial remodeling during PHT via suppressing the PDGF-BB/PDGFRβ signaling pathway, thereby offering novel insights into seek PHT treatment approaches.

CONCLUSIONS: Our findings revealed that metformin exerts its effects by activating the AMPK pathway, inhibiting the dedifferentiation of contractile VSMCs in the splanchnic arteries, and improving arterial remodeling, thereby ameliorating PHT and splanchnic hyperdynamic circulation in cirrhotic rats. *(Cell Mol Gastroenterol Hepatol 2025;19:101487; https://doi.org/10.1016/j.jcmgh.2025.101487)*

Keywords: Arterial Remodeling; Liver Cirrhosis; Phenotypic switching of VSMCs; Portal Hypertension; Splanchnic Hyperdynamic Circulation.

Globally, liver cirrhosis imposes a substantial burden on clinical practice and society, as it is characterized by the excessive deposition of extracellular matrix components (ECMs).[1] Portal hypertension (PHT) is known as a life-threatening complication of cirrhosis, closely associated with esophageal and gastric variceal bleeding and ascites.[2,3] The initial pathologic mechanism underlying PHT is drove by elevated intrahepatic resistance. Moreover, splanchnic hyperdynamic circulation is a crucial factor contributing to the exacerbation of PHT, including splanchnic arterial remodeling and vasodilation, ultimately resulting in a marked increase in portal venous inflow.[4] It is noteworthy that in advanced liver cirrhosis, the substantial deposition of ECM induces an irreversible pathologic progression in hepatic architecture, accompanied by refractory elevation of intrahepatic resistance. Consequently, ameliorating splanchnic hyperdynamic circulation emerges as an indispensable component of PHT therapeutic strategies.

Numerous previous studies have reported arterial wall thinning in both splanchnic and systemic circulations in liver cirrhosis with PHT.[5,6] In particular, the mesenteric arteries undergo arterial remodeling and vasodilation, exerting a remarkable impact on portal venous inflow. Due to the potential changes in protein levels critical for arterial function and integrity, arterial thinning may contribute to the impairment of arterial contractile responses and increased permeability, thereby facilitating vasodilation and ascites formation.[7] As previously reported in our study, phenotypic switching of vascular smooth muscle cells (VSMCs) emerged as an underlying mechanism for arterial remodeling and vasodilation in mesenteric arteries.[8] Nevertheless, the exact cellular and molecular mechanisms underlying arterial remodeling in cirrhosis have yet to be fully elucidated.

Interestingly, VSMCs exhibit remarkable plasticity throughout their lifecycle, contrasting with cardiomyocytes and skeletal muscle cells, as they do not exhibit terminal differentiation properties.[9] In response to various stimuli, VSMCs transform from a contractile to a synthetic phenotype. Synthetic VSMCs display enhanced proliferation and migration, characterized by increased expression of inflammatory mediators and decreased levels of contractile markers such as α-smooth muscle actin (α-SMA).[10] Indeed, phenotypic switching of VSMCs contributes to the remodeling and eventual rupture of the aneurysm.[11] Similarly, various mechanical and cellular stimuli have been observed to induce the phenotypic switching of VSMCs in cirrhosis with PHT. The shear force exerted on the vascular wall was remarkable increased in PHT, as evidenced.[12] Cirrhosis is always associated with chronic inflammation and the upregulation of growth factors, including platelet-derived growth factor-BB (PDGF-BB). Previous studies have demonstrated upregulation of PDGF-BB expression in serum during liver fibrosis, accompanied by excessively enhanced PDGF-BB/platelet-derived growth factor receptor-β

***Authors share co-first authorship.**

Abbreviations used in this paper: **ACC, acetyl-CoA carboxylase; αSMA, α-smooth muscle actin; ALT, alanine transaminase; AMPK, AMP-activated protein kinase; ANOVA, analysis of variance; AST, aspartate aminotransferase; BDL, bile duct ligation; CCK8, Cell Counting Kit-8; CI, cardiac index; CO, cardiac output; DMEM, Dulbecco's modified Eagle's medium; ECM, extracellular matrix component; ELISA, enzyme-linked immunosorbent assay; eNOS, endothelial nitric oxide synthase; FBS, fetal bovine serum; GAPDH, glyceraldehyde 3-phosphate dehydrogenase; H&E, hematoxylin and eosin; HR, heart rate; HSC, hepatic stellate cell; IF, immunofluorescence; IHC, Immunohistochemistry; IL, interleukin; MAP, mean arterial pressure; MMP9, matrix metalloproteinase-9; mTOR, mammalian target of rapamycin; PBS, phosphate-buffered saline; PDGF-BB, platelet-derived growth factor-BB; PDGFRβ, platelet-derived growth factor receptor-β; p-eNOS, phospho-endothelial nitric oxide synthase; PHT, portal hypertension; PP, portal pressure; p-VEGFR2, phospho-vascular endothelial growth factor receptor 2; RAS, renin angiotensin system; RNA-seq, RNA sequencing; RT-qPCR, quantitative reverse transcription polymerase chain reaction; SD, Sprague Dawley; SDS-PAGE, sodium dodecyl sulfate-polyacrylamide gel electrophoresis; SM22α, smooth muscle 22 alpha; SMA, superior mesenteric artery; SM-MHC, smooth muscle myosin heavy chain; SV, stroke volume; SVR, systemic vascular resistance; TBIL, total bilirubin; TNF-α, tumor necrosis factor-alpha; VEGFA, vascular endothelial growth factor A; VEGFR2, vascular endothelial growth factor receptor 2; VSMC, vascular smooth muscle cell.**

Most current article

2352-345X
https://doi.org/10.1016/j.jcmgh.2025.101487

(PDGFRβ) signaling, which stimulates proliferation and migration of hepatic stellate cells (HSCs).[13,14] Notably, PDGF-BB is known as one of the most potent mitogens to induce the dedifferentiation of VSMCs from a contractile to a synthetic phenotype.[15] However, the underlying mechanisms of how PDGF-BB promotes dedifferentiation of contractile VSMCs and mediates splanchnic arterial remodeling in liver cirrhosis remain poorly understood.

In recent years, a growing number of studies have focused on the increasing prevalence of diabetes mellitus among patients with cirrhosis.[16] Metformin, as a hypoglycemic agent, not only reduces blood glucose levels but also exhibits notable beneficial effects on mitigating hepatic fibrosis through multiple mechanisms.[17] Upon activation of AMP-activated protein kinase (AMPK) by metformin, it modulates the PDGF-BB-induced AKT/mammalian target of rapamycin (mTOR) signaling pathway, thereby inhibiting the proliferation and migration of HSCs.[18,19] Furthermore, metformin exhibits promising effects on the progression and rupture of intracranial aneurysm by inhibiting PDGF-BB-mediated arterial remodeling through the activation of the AMPK pathway.[20] Therefore, under the intervention of metformin, we have established *in vivo* models of bile duct ligation (BDL) rats with varying degrees of liver cirrhosis and *in vitro* experiments utilizing PDGF-BB-induced VSMCs as well as primary VSMCs from rats, aiming to investigate whether metformin affects the phenotype of VSMCs and improves arterial remodeling by activating AMPK and regulating PDGFR and its downstream pathways.

Results

Metformin Alleviates Liver Cirrhosis and Improves Liver Function in BDL Rats

In the long-term early metformin treatment group (Figure 1*A*), BDL rats exhibited severe disorder in the hepatic lobular structure. The hematoxylin and eosin (H&E) staining indicated that metformin treatment significantly ameliorated liver fibrosis, with a more intact hepatic lobule structure being observed. Similarly, results from Masson and Sirius Red staining confirmed that collagen deposition of BDL rats was significantly diminished following treatment with metformin, particularly with less damage to portal areas (Figure 2*A–C*). Furthermore, metformin also improved liver function in BDL rats, as evidenced by reduced levels of alanine transaminase (ALT), aspartate aminotransferase (AST), and total bilirubin (TBIL) (Figure 2*D–F*).

In the long-term late metformin treatment group (Figure 1*B*), H&E, Masson, and Sirius Red staining revealed a significant exacerbation of liver cirrhosis after 6 weeks of BDL, which was characterized by notable aggravated hepatocyte loss, increased collagen deposition, particularly severe destruction around the portal areas, and more evident bile stasis and dilated bile ducts (Figure 2*G*). Quantitative analysis of Masson and Sirius Red staining confirmed a significant augmentation in collagen deposition in rats following 6 weeks of BDL, with partial amelioration by metformin (Figure 2*H–I*). After metformin treatment, a partial amelioration in the levels of ALT and AST was observed in rats with advanced cirrhosis. Nevertheless, no significant difference was observed in the TBIL levels. (Figure 2*J–L*). These results demonstrated that metformin alleviated liver cirrhosis but provided partial improvement in advanced stages due to severe damage to hepatic structure and collagen deposition.

Metformin Ameliorates Portal Pressure and Splanchnic Hyperdynamic Circulation in Cirrhotic Rats

We further investigated the impact of metformin on systemic and splanchnic hemodynamics in cirrhotic rats at 4- and 6-weeks post BDL. It was observed that in the early metformin treatment group, there was a slight increase in body weight of rats compared to the BDL group. Metformin treatment significantly reduced cardiac load in BDL rats, as demonstrated by improved cardiac output (CO) and cardiac

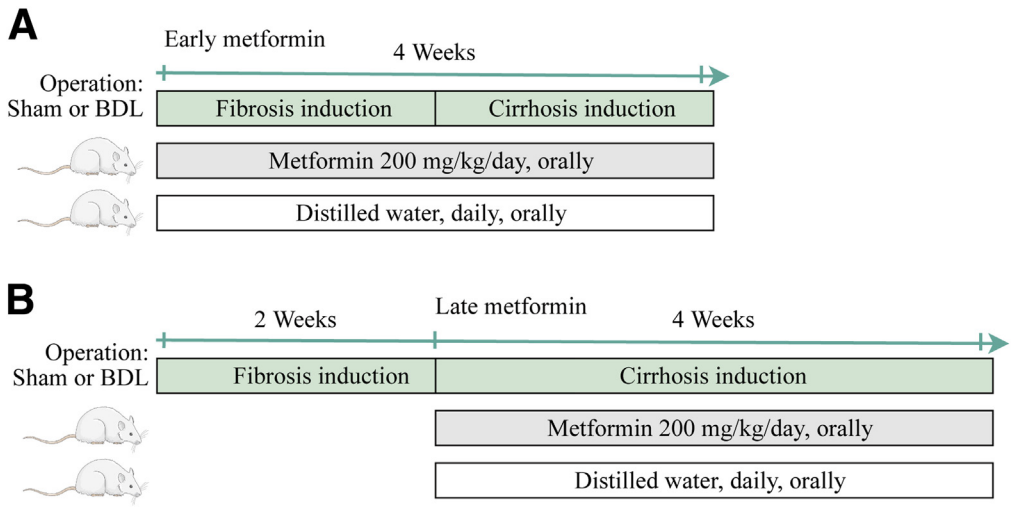

Figure 1. Construction of animal model of liver cirrhosis and metformin administration. (*A*) In the long-term early metformin treatment group, either metformin or vehicle was administered starting immediately on the first day following BDL surgery and continued for 4 weeks. (*B*) In the long-term late metformin group, treatment with either metformin or vehicle commenced on the 15th day post-BDL and continued for 4 weeks.

index (CI), along with an elevation in systemic vascular resistance (SVR). Notably, splanchnic hyperdynamic circulation was remarkably alleviated in metformin-treated BDL rats, marked by reduced portal pressure (PP), decreased superior mesenteric artery (SMA) flow, and increased SMA resistance (Table 1).

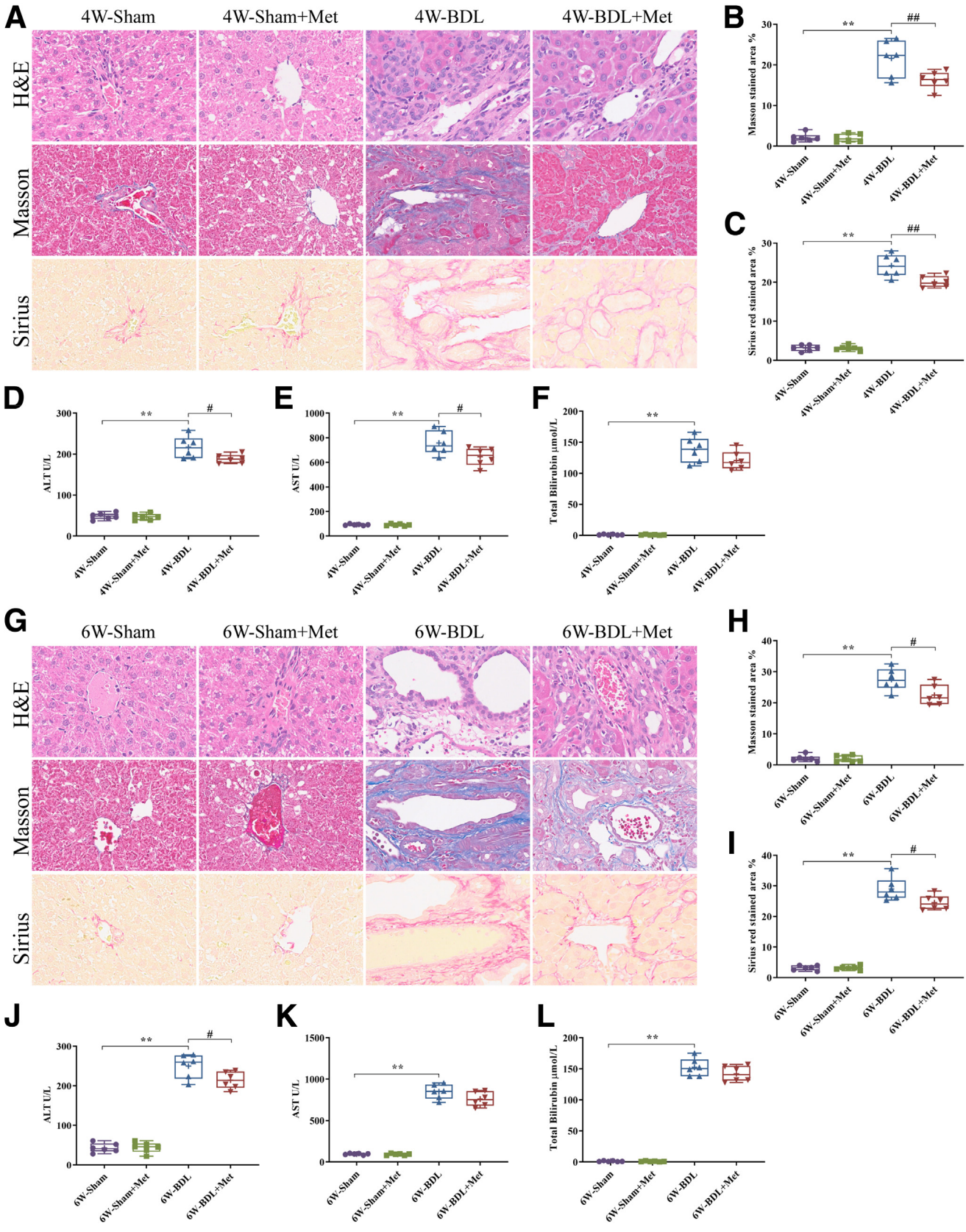

Table 1. BW and Hemodynamics

Characteristics	Sham	Sham + Met	BDL	BDL + Met
BW, *g*	395.8 ± 16.6	395.5 ± 8.2	360.8 ± 17.4[a]	377.0 ± 8.4
MAP, *mmHg*	113.3 ± 6.8	115.8 ± 6.7	93.2 ± 6.3[a]	95.5 ± 6.0
PP, *mmHg*	6.7 ± 1.4	6.2 ± 1.5	15.3 ± 1.9[a]	11.8 ± 3.2[b]
HR, *beats/min*	303 ± 10	302 ± 13	338 ± 24	335 ± 37
SV, *mL/beats*	0.52 ± 0.06	0.51 ± 0.04	0.66 ± 0.05[a]	0.53 ± 0.06[c]
CO, *mL/min*	157.3 ± 17.2	155.2 ± 15.8	221.0 ± 14.0[a]	179.4 ± 32.9[b]
CI, *mL/min/100 g*	39.7 ± 3.9	39.2 ± 3.4	61.4 ± 5.6[a]	47.6 ± 9.1[c]
SVR, *mmHg/mL/min/100 g*	2.9 ± 0.4	3.0 ± 0.2	1.5 ± 0.1[a]	2.1 ± 0.4[b]
SMA flow, *mL/min/100 g*	2.6 ± 0.6	2.4 ± 0.5	6.1 ± 0.5[a]	4.1 ± 0.6[c]
SMA resistance, *mmHg/mL/min/100 g*	43.0 ± 9.8	46.5 ± 9.4	13.0 ± 1.8[a]	21.3 ± 4.7[c]

BDL, bile duct ligation; BW, body weight; CI, cardiac index; CO, cardiac output; HR, heart rate; MAP, mean arterial pressure; Met, metformin; PP, portal pressure; SMA, superior mesenteric artery; SV, stroke volume; SVR, systemic vascular resistance.
[a]Sham group vs BDL group; $P < .01$.
[b]BDL group vs BDL + Met group; n = 6; 1-way analysis of variance; mean ± standard deviation; $P < .05$.
[c]BDL group vs BDL + Met group; n = 6; 1-way analysis of variance; mean ± standard deviation; $P < .01$.

Despite the irreversible nature of advanced cirrhosis at 6 weeks post BDL, we also observed a significant reduction in PP in metformin-treated BDL rats, along with a notable decrease in SMA flow and an improvement in SMA resistance. Moreover, metformin treatment partially alleviated the cardiac load in BDL rats, leading to a decrease in both CO and CI, although this change did not reach statistical significance. Nevertheless, it was accompanied by a significant increase in SVR (Table 2). Collectively, these findings suggested that metformin exhibited beneficial effects on PHT and splanchnic hyperdynamic circulation in both early and late stages of liver cirrhosis.

Metformin Relieves Chronic Inflammation and Suppressed Macrophage Infiltration in the Mesentery of BDL Rats

Chronic inflammation caused by cirrhosis is a crucial factor promoting angiogenesis and vascular remodeling. Following metformin treatment, a notable reduction was observed in the serum levels of inflammatory factors interleukin (IL)-1β, IL-6, and tumor necrosis factor-alpha (TNF-α) in rats at 4 weeks post-BDL surgery (Figure 3*A*). Similarly, despite the aggravation of liver cirrhosis in BDL rats at 6 weeks post-surgery, metformin treatment continued to attenuate the expression of IL-1β, IL-6, and TNF-α in the advanced cirrhotic rats (Figure 3*B*). Subsequently, immunofluorescence staining of mesenteric tissue revealed a significant increase in infiltrating CD68-positive cells in BDL rats. Early treatment with metformin led to a significant reduction in the number of CD68-positive cells, indicating a mitigation of macrophage infiltration (Figure 3*C–D*). Similarly, at 6 weeks post-BDL surgery, a significant increase in the abundance of CD68-positive cells within the mesenteric tissue was observed. Notably, metformin treatment remarkably reduced the number of CD68-positive cells, thereby ameliorating macrophage infiltration and alleviating local inflammation in BDL rats (Figure 3*E–F*). Therefore, metformin effectively alleviated systemic and mesenteric inflammation, and reduced macrophage infiltration in BDL rats, which potentially inhibited the inflammation driving angiogenesis and arterial remodeling.

Metformin Suppresses Mesenteric Angiogenesis in BDL Rats

Angiogenesis triggers the formation of collateral circulation in cirrhosis, playing a crucial role in the progression of PHT. Following BDL surgery for 4 weeks, immunofluorescence (IF) results demonstrated a significant upregulation of CD31 expression in the mesentery of BDL rats, indicating a marked increase in angiogenesis. However, the early metformin treatment effectively suppressed vascular proliferation in the mesentery (Figure 4*A–B*). Similarly, at 6 weeks post-BDL surgery, IF results revealed a more pronounced elevation in CD31 expression and a significantly higher quantity of newly developed blood vessels in the mesentery of rats. Later, the administration of metformin to BDL rats substantially suppressed angiogenesis in the mesentery. (Figure 4*C–D*). Moreover, in both early and late

Figure 2. (***See previous page***). **Metformin alleviates the liver fibrosis and function in BDL rats.** (*A*) Representative images of H&E, Masson's trichrome, and Sirius red staining of liver in rats at 4 weeks post-BDL. (*B*) Quantitative analysis of Masson's trichrome staining. (*C*) Quantitative analysis of Sirius red staining. (*D–F*) The expression levels of ALT, AST, and TBIL in serum. (*G*) Representative image of H&E, Masson's trichrome, and Sirius red staining of liver in rats at 6 weeks post-BDL. (*H*) Quantitative analysis of Masson's trichrome staining. (*I*) Quantitative analysis of Sirius red staining. (*J–L*) The expression levels of ALT, AST, and TBIL in serum. n = 6 rats per group; 1-way ANOVA; mean ± standard deviation; $^{\#,*}P < .05$; $^{\#\#,**}P < .01$.

Table 2. BW and Hemodynamics

Characteristics	Sham	Sham + Met	BDL	BDL + Met
BW, *g*	410.8 ± 16.5	412.2 ± 6.3	369.2 ± 20.8[a]	385.8 ± 10.9
MAP, *mmHg*	118.7 ± 7.5	117.3 ± 8.3	84.7 ± 6.0[a]	89.3 ± 7.0
PP, *mmHg*	6.8 ± 1.2	6.5 ± 1.9	18.5 ± 2.8[a]	14.5 ± 2.7[b]
HR, *beats/min*	300 ± 13	301 ± 18	365 ± 29[a]	351 ± 25
SV, *mL/beats*	0.50 ± 0.06	0.53 ± 0.04	0.71 ± 0.07[a]	0.64 ± 0.09[c]
CO, *mL/min*	150.8 ± 22.5	158.2 ± 20.8	252.6 ± 24.2[a]	225.4 ± 34.5
CI, *mL/min/100 g*	36.8 ± 6.0	38.4 ± 5.1	68.7 ± 8.2[a]	58.5 ± 9.8
SVR, *mmHg/mL/min/100 g*	3.3 ± 0.7	3.1 ± 0.5	1.3 ± 0.2[a]	1.6 ± 0.3[b]
SMA flow, *mL/min/100 g*	2.7 ± 0.7	2.7 ± 0.5	7.2 ± 0.8[a]	5.1 ± 0.7[c]
SMA resistance, *mmHg/mL/min/100 g*	43.3 ± 10.7	42.2 ± 6.8	9.3 ± 1.3[a]	14.8 ± 2.0[c]

BDL, bile duct ligation; BW, body weight; CI, cardiac index; CO, cardiac output; HR, heart rate; MAP, mean arterial pressure; Met, metformin; PP, portal pressure; SMA, superior mesenteric artery; SV, stroke volume; SVR, systemic vascular resistance.
[a]Sham group vs BDL group; $P < .01$.
[b]BDL group vs BDL + Met group; n = 6; 1-way analysis of variance; mean ± standard deviation; $P < .05$.
[c]BDL group vs BDL + Met group; n = 6; 1-way analysis of variance; mean ± standard deviation; $P < .01$.

stages of cirrhosis, the expression of vascular endothelial growth factor A (VEGFA) was significantly upregulated in both serum and mesentery. However, metformin treatment resulted in a significant decrease in VEGFA expression in BDL rats (Figure 4*E–F*). Consistent with the expression of VEGFA in serum and mesentery, we observed a significant increase in the expression of p-VEGFR2 in mesenteric arteries of rats with cirrhosis at different stages. Indeed, both early and late metformin treatment effectively suppressed the expression of phospho-vascular endothelial growth factor receptor 2 (p-VEGFR2) in the mesentery (Figure 4*G–H*). Together, metformin inhibited mesenteric angiogenesis in early and late stages of cirrhosis by suppressing VEGFR2 signaling, thereby attenuating the progression of PHT.

Metformin Upregulates Arterial Contractile Proteins Expression and Mitigates Mesenteric Arterial Remodeling in BDL Rats

Arterial remodeling is a pivotal driving factor contributing to splanchnic hyperdynamic circulation in cirrhosis. SMA remodeling in the rats 4 weeks post-BDL was marked by decreased arterial wall thickness, notably thinning of the smooth muscle layer in the tunica media, accompanied by arterial dilation. Following early treatment with metformin, a substantial restoration of tunica media smooth muscle layer thickness was observed (Figure 5*A–B*). Similarly, at 6 weeks post-BDL surgery, there was a more serious reduction in the smooth muscle layer of SMA, leading to exacerbated arterial remodeling. It was further confirmed that metformin effectively inhibits SMA dilation and arterial remodeling in cirrhotic rats (Figure 5*C–D*). Moreover, these findings were consistent with the suppressed expression of phospho-endothelial nitric oxide synthase (p-eNOS) in the SMA of BDL rats following both early and late metformin treatment (Figure 5*E–F*).

VSMCs in mature animal vascular display a contractile phenotype and express various hallmark contractile proteins, including α-SMA and smooth muscle 22 alpha (SM22α).[21] At 4 weeks post-BDL, the SMA tunica media exhibited thinning, accompanied by a significant reduction in the expression of contractile proteins α-SMA and SM22α. Conversely, early metformin treatment led to a more intact tunica media structure of the SMA wall, along with a noticeable elevation in the expression levels of α-SMA and SM22α (Figure 5*G and I*). Furthermore, with the progression of cirrhosis, a more significant thinning of the tunica media at 6 weeks post-BDL was observed, accompanied by markedly reduced expression of α-SMA and SM22α. Notably, following metformin treatment, there was a significant increase in the thickness of the tunica media at 6 weeks post-BDL, accompanied by a notable elevation in the expression of α-SMA and SM22α, whereas arterial remodeling was suppressed (Figure 5*H and J*). Taken together, these results suggested that metformin effectively increased the expression of arterial contractile proteins, leading to improvements in arterial tunica media thinning and SMA dilation in both early and late-stage cirrhotic rats. These effects may not solely rely on the amelioration of cirrhosis in mitigating arterial remodeling in BDL rats.

Blocking the PDGFRβ Pathway to Inhibit Dedifferentiation of Contractile VSMCs Improves Arterial Remodeling in BDL Rats

Phenotypic switching of VSMCs from a contractile to a synthetic phenotype represents a hallmark event in vascular remodeling,[22] with the upregulation of inflammatory mediators and the decrease of contractile-related proteins. To further investigate the underlying mechanisms of arterial remodeling in cirrhotic rats, we first assessed the expression of inflammation-related genes. The quantitative reverse transcription polymerase chain reaction (RT-qPCR) revealed

a significant upregulation of IL-1β, IL-6, TNF-α, and matrix metalloproteinase-9 (MMP9) expression in the SMA at 4 weeks post-BDL. Similarly, at 6 weeks post-BDL, a more pronounced increase in IL-1β, IL-6, TNF-α, and MMP9 expression was observed. Following early and late metformin treatment, there was a marked decrease in the

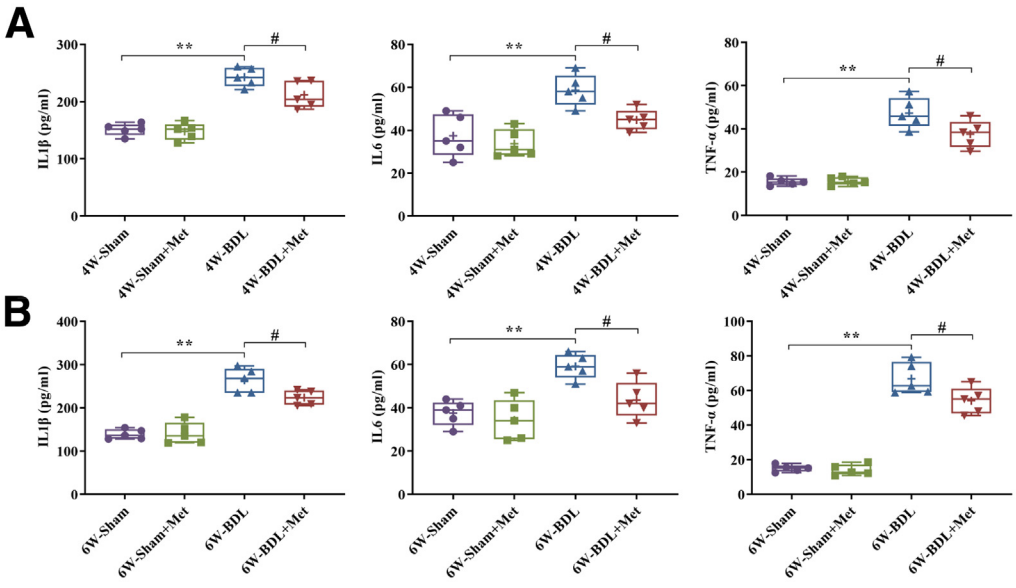

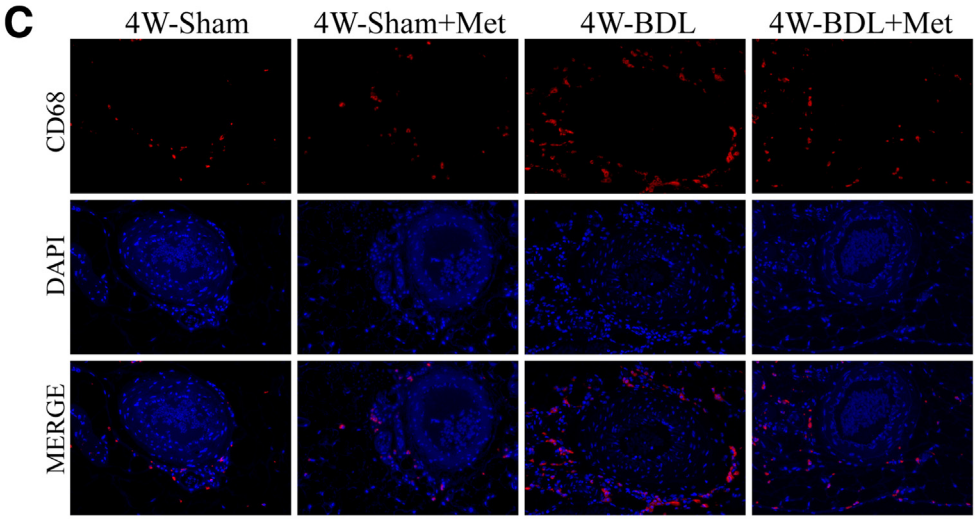

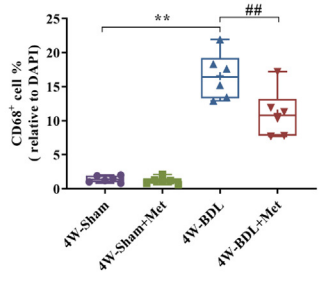

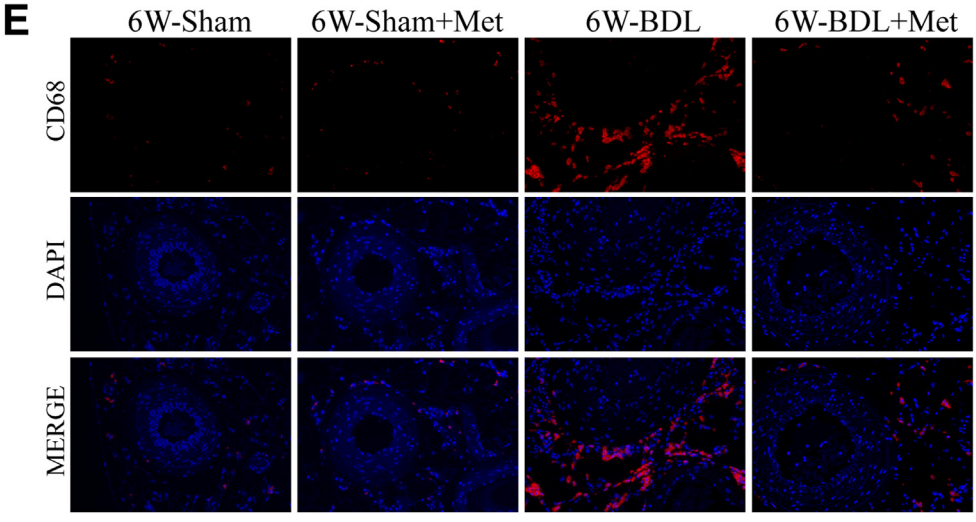

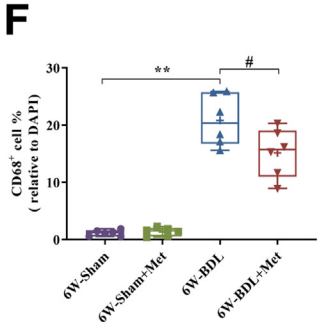

expression levels of these inflammatory markers (Figure 6*A–B*). In addition, we confirmed the down-regulation of contractile proteins α-SMA and SM22α expression in the SMA at 4 and 6 weeks post-BDL. Interestingly, metformin treatment reversed the decreased expression of α-SMA and SM22α in the SMA, regardless of the stage of liver fibrosis (Figure 6*C–D*).

Our previous study has revealed that the dedifferentiation of VSMCs in the mesenteric arteries of BDL rats may serve as a potential mechanism contributing to arterial remodeling.[8] Based on our RNA sequencing (RNA-seq) data, the expression of PDGFRβ, a significantly differentially expressed gene, was significantly up-regulated in BDL rats (Figure 6*E*). PDGF-BB is recognized as a key mediator that triggers VSMC phenotypic switching via its activation of PDGFRβ. We found a significant increase in the expression levels of PDGF-BB in the serum and mesentery of BDL rats at 4 and 6 weeks post-BDL. Following early and late administration of metformin, the expression levels of PDGF-BB in BDL rats decreased partially but remained elevated compared with the sham group (Figure 6*F*). Correspondingly, there was a significant elevation in the expression levels of p-PDGFRβ in the SMA at 4 and 6 weeks post-BDL (Figure 6*G–H*). Upon PDGFRβ phosphorylation leading to downstream signaling pathway activation, Western blot analysis revealed a significant increase in p-mTOR expression in SMA of BDL rats. Notably, activation of the AMPK pathway in the SMA of BDL rats was induced by metformin, as evidenced by an increase in p-AMPK and p-ACC expression, subsequently resulting in a marked suppression of p-mTOR expression (Figure 6*I–J*). Therefore, it was suggested that the downstream signaling pathway of PDGFRβ was blocked by metformin through the activation of AMPK, leading to the inhibition of the dedifferentiation of contractile VSMCs, consequently improving arterial remodeling in BDL rats.

Metformin Modulates the Proliferation and Migration Capacity of A7r5 Cells Mediated by PDGF-BB

VSMC proliferation and migration are closely associated with synthetic phenotype. Our *in vitro* experiments investigated the inhibitory effect of metformin on the phenotypic switching of VSMCs induced by PDGF-BB. First, our results revealed that no cytotoxicity was observed when A7r5 cells were exposed to metformin at concentrations below 5mM (Figure 7*A*). As shown in Figure 7*B*, the proliferation of A7r5 cells was significantly enhanced by PDGF-BB, whereas metformin exhibited an inhibitory effect. Conversely, Compound C, an AMPK inhibitor, reversed the inhibitory effect of metformin, resulting in the restoration of proliferation in A7r5 cells. Furthermore, cell scratch assay revealed that PDGF-BB significantly enhanced the migration of A7r5 cells, resulting in a marked reduction in scratch width. Metformin suppressed PDGF-BB-induced cell migration. However, the inhibitory effect of metformin was reversed by an AMPK inhibitor (Figure 7*C and E*). Similarly, the transwell experiment revealed that PDGF-BB enhanced the migratory capacity of A7r5 cells, resulting in a significant increase in the number of cells migrating into the chamber. However, metformin inhibited the migration of A7r5 cells, whereas the AMPK inhibitor exhibited a reversing effect. (Figure 7*D and F*). Therefore, the PDGF-BB-induced phenotypic switching of VSMCs was suppressed by metformin, inhibiting the proliferation and migration capabilities of A7r5 cells.

Activation of AMPK Inhibits the PDGF-BB-induced Phenotypic Switching in A7r5 Cells

We observed that PDGF-BB induced a reduction in α-SMA expression in A7r5 cells, concomitant with elevated expression levels of TNF-α and MMP9, indicative of the phenotypic switching from contractile VSMCs into synthetic cells. On the contrary, the expression of α-SMA was upregulated by metformin in A7r5 cells, whereas the expression of TNF-α and MMP9 was decreased. Notably, these effects were reversed by the compound C (Figure 8*A–B*). IF analysis revealed that, compared with administration of PDGF-BB alone, the expression of p-AMPK in A7r5 cells was increased by metformin. However, the activation of the AMPK pathway by metformin was significantly inhibited by Compound C (Figure 8*C–D*). Furthermore, Western blot analysis confirmed that PDGF-BB promoted the phosphorylation of PDGFRβ and activated downstream signaling pathway, increasing mTOR phosphorylation. However, activation of the AMPK by metformin significantly reduced the expression of p-mTOR in A7r5 cells. Interestingly, inhibition of AMPK resulted in upregulation of p-mTOR expression, thereby reversing the inhibitory effect of metformin on the downstream signaling pathway of PDGFRβ (Figure 8*E–F*). Collectively, these results revealed that metformin suppressed the phenotypic switching of A7r5 cells by activating AMPK to block the downstream pathways of PDGFRβ.

Activation of AMPK Alleviates the Phenotypic Switching of Primary VSMCs From Cirrhotic Rats

We further explored the mechanism underlying the effect of metformin on primary VSMCs from cirrhotic rats. The expression of contractile protein α-SMA was significantly down-regulated in primary VSMCs from BDL rats, accompanied by

Figure 3. (***See previous page***). **Metformin inhibits chronic inflammation and macrophage infiltration in the mesentery of BDL rats.** (*A–B*) Metformin suppressed the expression of inflammatory factors in rats at 4 and 6 weeks post-BDL. (*C*) The early treatment with metformin inhibited macrophage infiltration in the mesentery of BDL rats. (*D*) Quantitative analysis of CD68 positive macrophages in rats at 4 weeks post-BDL. (*E*) The late treatment with metformin inhibited macrophage infiltration in the mesentery of BDL rats. (*F*) Quantitative analysis of CD68 positive macrophages in rats at 6 weeks post-BDL. n = 5–6 rats per group; 1-way ANOVA; mean ± standard deviation; $^{\#,*}P < .05$; $^{\#\#,**}P < .01$.

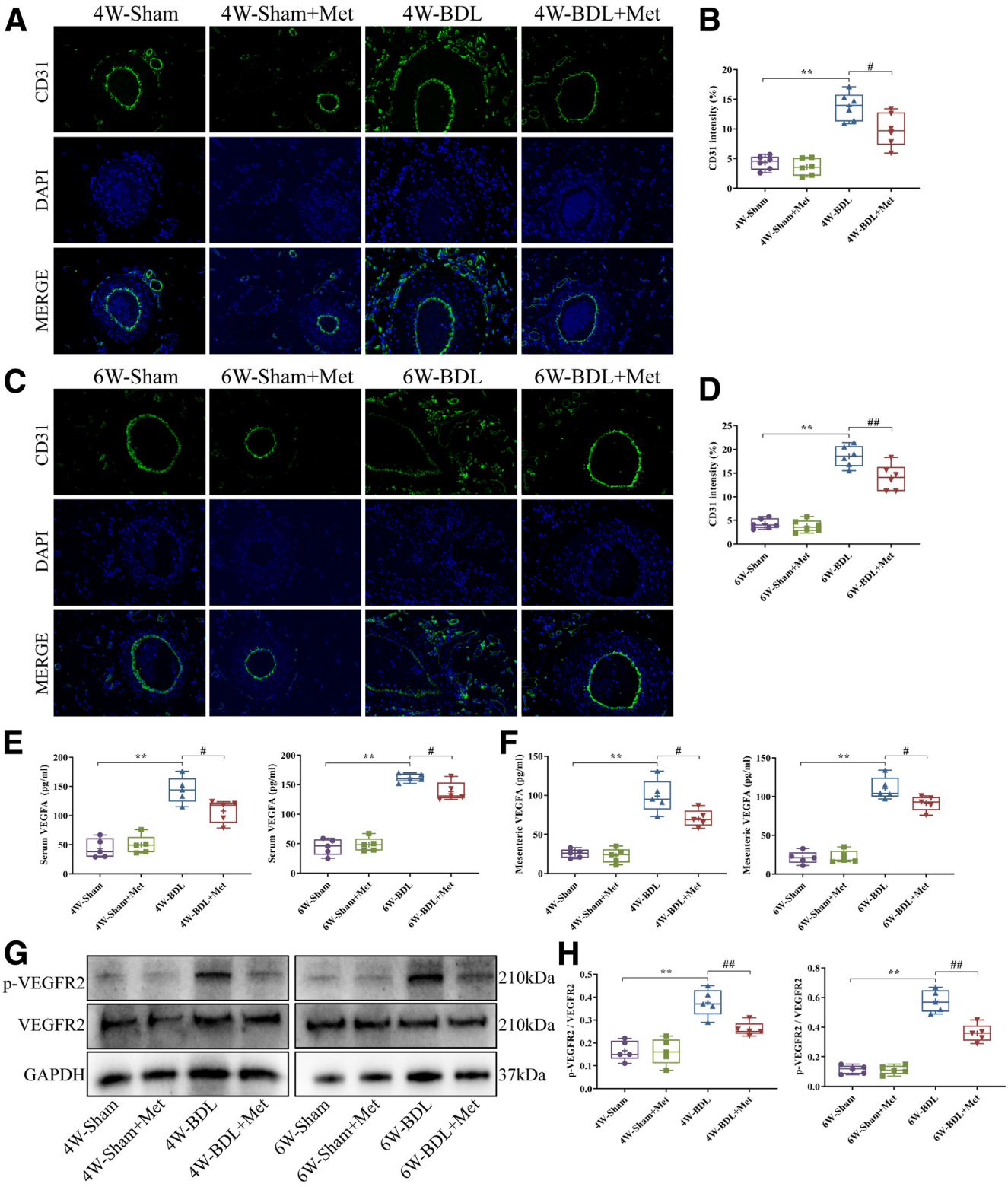

Figure 4. Metformin inhibits mesenteric angiogenesis in BDL rats. (*A*) The early metformin treatment suppressed mesenteric angiogenesis in BDL rats. (*B*) Quantitative analysis of mesenteric CD31 in rats at 4 weeks post-BDL. (*C*) The late metformin treatment suppressed mesenteric angiogenesis in BDL rats. (*D*) Quantitative analysis of mesenteric CD31 in rats at 6 weeks post-BDL. (*E–F*) The expression levels of VEGFA in serum and mesentery. (*G*) Metformin inhibited the expression of p-VEGFR2 in mesentery of BDL rats. (*H*) Quantitative analysis of p-VEGFR2/VEGFR2. n = 5–6 rats per group; 1-way ANOVA; mean ± standard deviation; $^{\#,*}P < .05$; $^{\#\#,**}P < .01$.

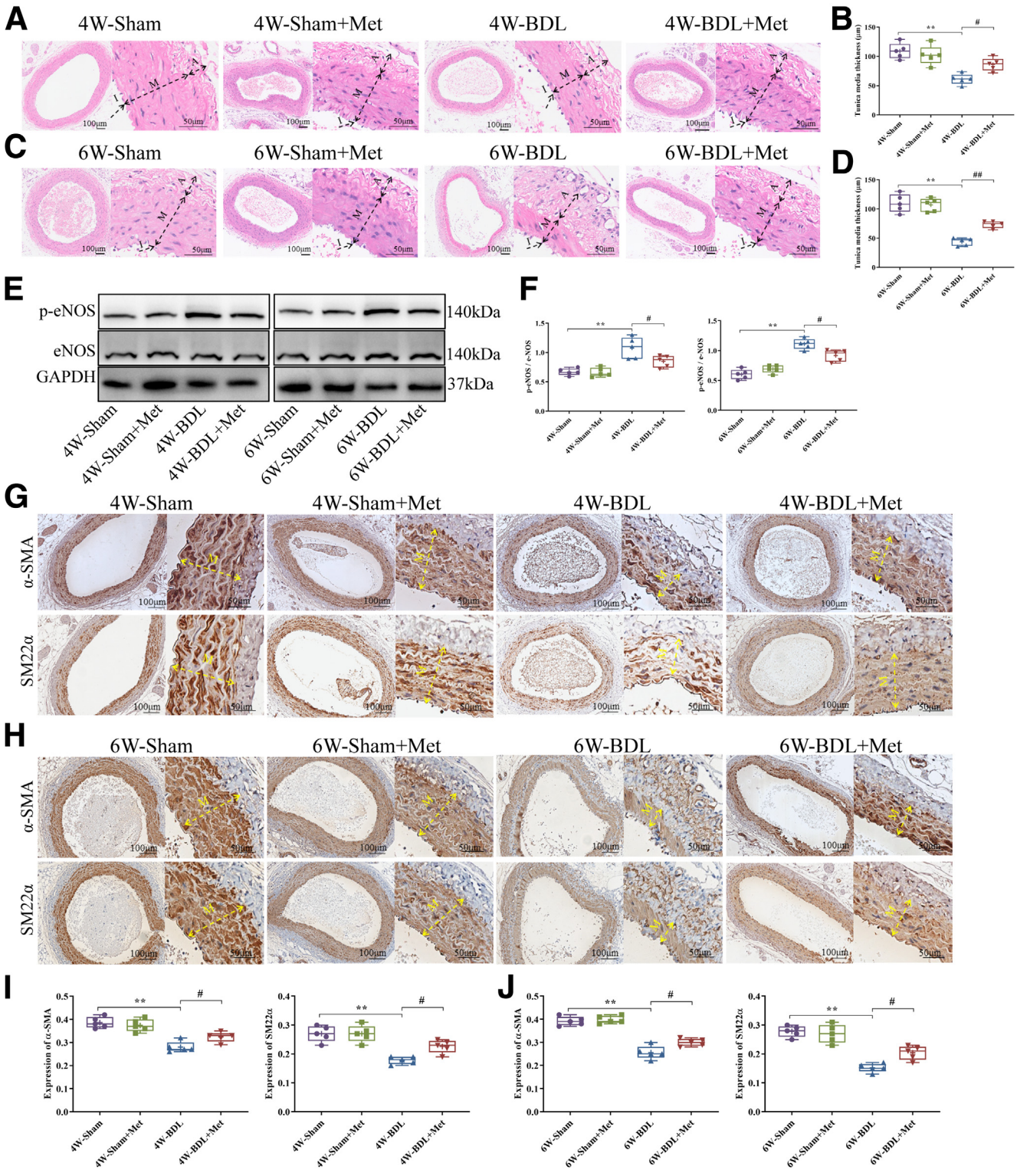

Figure 5. Metformin improves mesenteric arterial remodeling and increases contractile proteins expression in BDL rats. (*A*) The early metformin treatment improved the SMA dilation and arterial remodeling in BDL rats. (*B*) Tunica media thickness of SMA in rats at 4 weeks post-BDL. (*C*) The late metformin treatment improved the SMA dilation and arterial remodeling in BDL rats. (*D*) Tunica media thickness of SMA in rats at 6 weeks post-BDL. (*E*) Metformin inhibited the expression of p-eNOS in mesentery of BDL rats. (*F*) Quantitative analysis of p-eNOS/eNOS. (*G–H*) The early and late metformin treatment increased the expression of contractile proteins α-SMA and SM22α in tunica media of SMA in BDL rats. (*I–J*) Quantitative analysis of α-SMA and SM22α in rats at 4 and 6 weeks post-BDL. A, tunica adventitia; I, tunica intima; M, tunica media; n = 5–6 rats per group; 1-way ANOVA; mean ± standard deviation; $^{\#,*}P < .05$; $^{\#\#,**}P < .01$.

upregulation of TNF-α and MMP9, similar to the induction of synthetic phenotype in A7r5 cells by PDGF-BB. Our results demonstrated that the expression of α-SMA was upregulated by metformin, whereas TNF-α and MMP9 were downregulated in primary VSMCs. Importantly, Compound C effectively reversed the effects of metformin (Figure 9*A–B*). Furthermore,

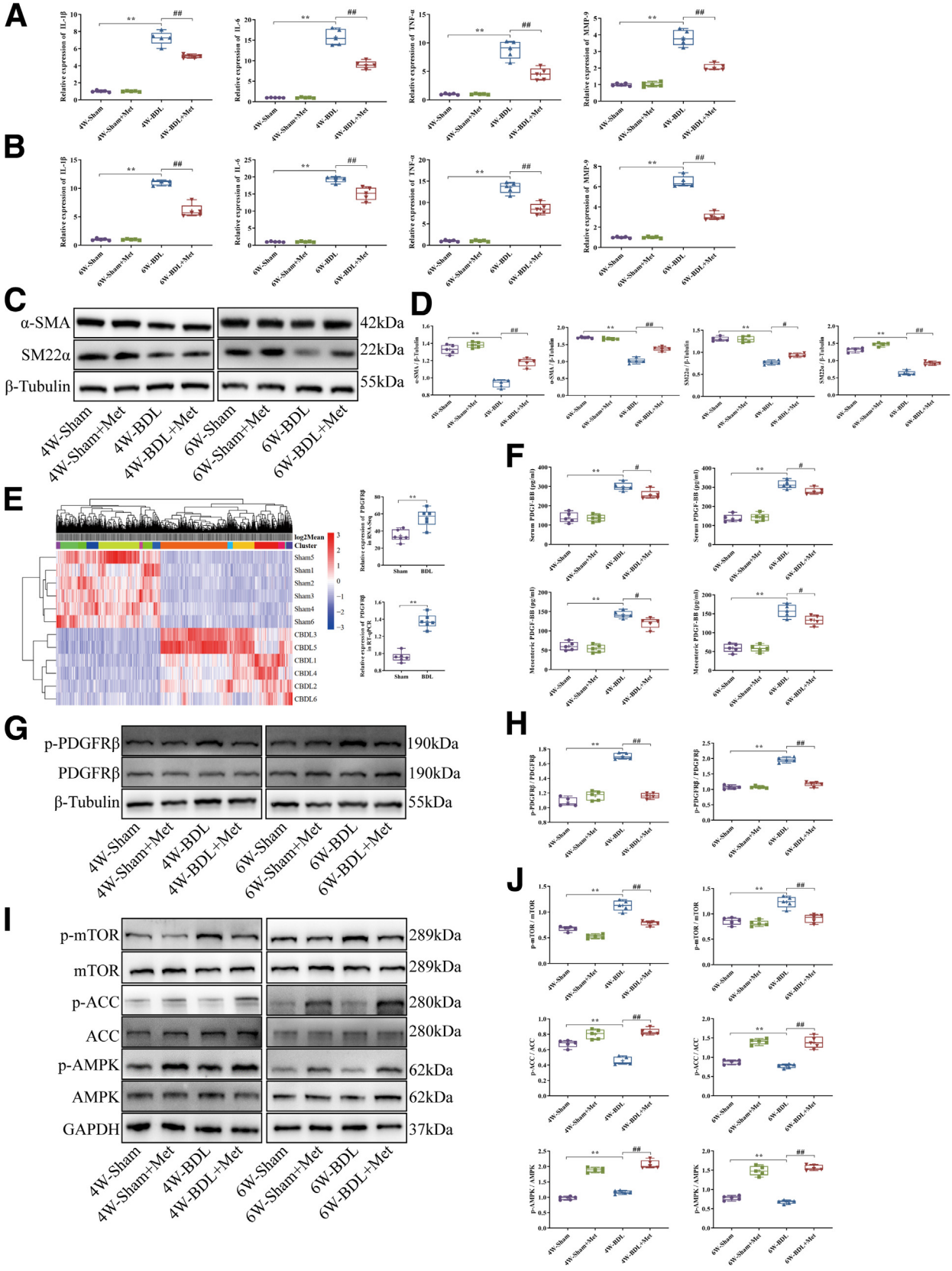

immunofluorescence analysis confirmed a decrease in the expression of contractile protein α-SMA in primary VSMCs from BDL rats, which was upregulated by metformin. Subsequent treatment with Compound C led to a decrease in α-SMA expression (Figure 9*C*–*D*). In addition, the expression of p-AMPK was significantly increased in primary VSMCs following treatment with metformin, whereas the AMPK pathway was inhibited by Compound C, resulting in the downregulation of p-AMPK expression (Figure 9*E*–*F*). Taken together, these findings confirmed that metformin enhanced the expression of contractile proteins by activating AMPK, thereby inhibiting the dedifferentiation of contractile primary VSMCs from cirrhotic rats.

Discussion

In liver cirrhosis, increased intrahepatic vascular resistance and hyperdynamic splanchnic circulation are dominant factors contributing to the maintenance and exacerbation of PHT.[23] Specifically, arterial remodeling and angiogenesis are key pathophysiologic mechanisms driving the hyperdynamic splanchnic circulation. Indeed, in the advanced stages of cirrhosis, the liver fibrosis becomes irreversible, leading to persistent and intractable increases in intrahepatic vascular resistance. Faced with this challenge, the inhibition of arterial remodeling and dilation to alleviate the hyperdynamic splanchnic circulation may emerge as an indispensable component of treatment strategies for advanced liver cirrhosis.[24]

In our study, we innovatively designed a therapeutic intervention of metformin administration in rats with different stages of liver cirrhosis. Our results demonstrated that metformin exhibited beneficial effects on liver cirrhosis and PHT in rats at 4- and 6-weeks post-BDL. Especially in the advanced stages of liver cirrhosis, metformin continued to ameliorate PHT and splanchnic hyperdynamic circulation in BDL rats, manifested by reduced PP and CO and decreased SMA flow, accompanied by improvements in SVR and SMA resistance. Chronic inflammation in BDL rats was alleviated by metformin, which might inhibit the driving factors of angiogenesis and arterial remodeling. Notably, in cirrhotic rats, SMA dilation and arterial wall thinning were potently alleviated by metformin. Specifically, we found that metformin improved arterial remodeling in BDL rats by inhibiting the dedifferentiation of contractile VSMCs through activating AMPK to block the downstream pathway of PDGFRβ. Furthermore, the *in vitro* cell experiments confirmed that metformin inhibited the phenotypic switching of A7r5 cells and primary VSMCs by activating AMPK, thereby enhancing the expression of contractile proteins. Unlike other previous studies, our study is the first to elucidate the potential mechanism of arterial remodeling in liver cirrhosis from the perspective of VSMCs (Figure 10). These findings may inspire novel therapeutic approaches for advanced liver cirrhosis characterized by irreversible intrahepatic vascular resistance, with the aim of ameliorating PHT and its life-threatening vascular complications.

Liver cirrhosis is characterized by chronic systemic inflammation, inducing the release of inflammatory mediators. These mediators subsequently recruit inflammatory cells, exacerbating local vascular inflammation, thus initiating neovascularization and arterial remodeling.[25] In our study, we observed a reduction in the expression levels of inflammatory cytokines IL-1β, IL-6, and TNF-α following metformin treatment in BDL rats. Additionally, a noteworthy mitigation of macrophage infiltration was observed in the mesenteric tissue of BDL rats. Much evidence has found that the crucial role of macrophage-mediated inflammatory responses is as primary initiators of angiogenesis.[26] Consistent with these findings, our study observed that the administration of metformin to BDL rats markedly suppressed angiogenesis, as evidenced by a significant decrease in CD31 expression within the mesentery. Furthermore, VEGFR2 is recognized as the key signaling receptor for VEGF and plays a pivotal role in facilitating angiogenesis in cirrhosis.[27] Metformin administration in BDL rats resulted in a reduction of p-VEGFR2 expression, indicating inhibition of the VEGFR2 pathway and subsequent suppression of angiogenesis. Hence, based on our findings, metformin demonstrated the ability to inhibit inflammation and reduce macrophage infiltration in both early and advanced stages of liver cirrhosis. This contributed to maintaining vascular structure and stability and reducing the formation of splanchnic vascularity in PHT.

PHT induces the formation of collateral vessels and arterial vasodilation in both splanchnic and systemic circulations, aggravating the condition. Specifically, arterial remodeling and vasodilation in the splanchnic circulation during cirrhosis contribute to increased blood flow to the portal vein. Previous studies have confirmed that solely mitigating collateral vessel formation would not suffice to alleviate PHT. It is crucial to inhibit arterial remodeling in splanchnic circulation to concomitantly reduce blood flow to the portal vein.[23,24] In this study, early administration of metformin reduced PP in BDL rats, as well as decreased rat CO and SMA flow, while improving SVR and SMA resistance, thereby alleviating PHT and splanchnic hyperdynamic circulation. It is noteworthy that late-stage metformin treatment, although challenging to reverse the severity of liver fibrosis, still exhibited similar effects by reducing SMA flow

Figure 6. (***See previous page***). **Activation of AMPK blocks PDGF-BB/PDGFRβ pathway, inhibiting the dedifferentiation of contractile VSMCs.** (*A*–*B*) The relative expression levels of IL-1β, IL-6, TNF-α, and MMP9 in SMA at 4 and 6 weeks post-BDL. (*C*–*D*) The expression levels of contractile proteins in SMA at 4 and 6 weeks post-BDL. (*E*) The expression of PDGFRβ, a differentially expressed gene in the mesenteric artery in the RNA-seq of BDL rats. (*F*) The expression level of PDGF-BB in serum and mesentery. (*G*) Metformin inhibited the expression of p-PDGFRβ in BDL rats. (*H*) Quantitative analysis of p-PDGFRβ/PDGFRβ. (*I*–*J*) Metformin activated AMPK and ACC and inhibited the expression of p-mTOR in BDL rats. n = 5–6 rats per group; 1-way ANOVA or Student *t*-test was applied; mean ± standard deviation; $^{\#,*}P < .05$; $^{\#\#,**}P < .01$.

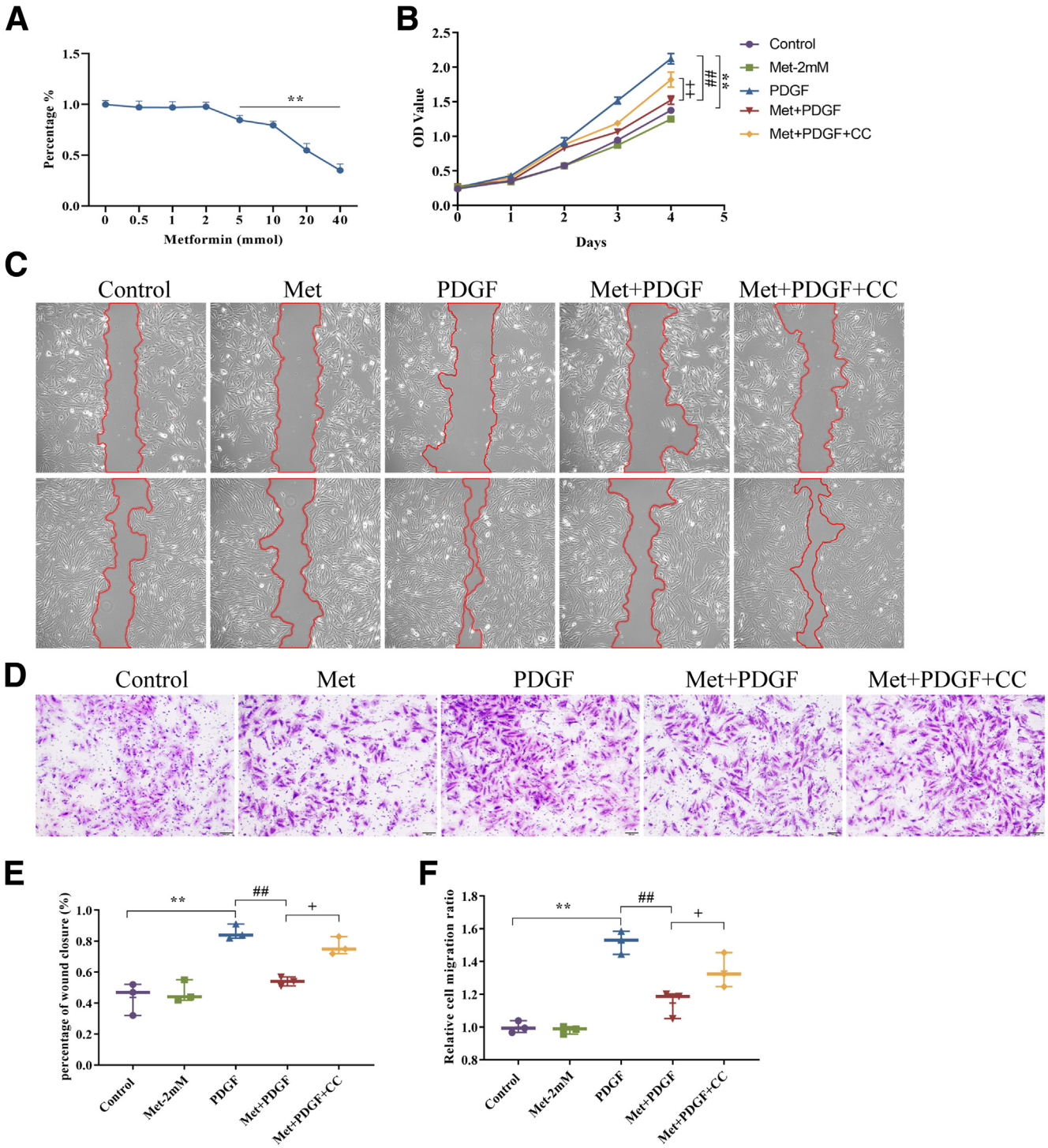

Figure 7. The regulation of metformin on PDGF-BB-induced proliferation and migration of A7r5 cells. (*A*) The metformin cytotoxicity of A7r5 cells for 48 hours. (*B*) Metformin inhibited the PDGF-BB-induced proliferation of A7r5 cells. (*C*) Scratch assay of A7r5 cells. (*D*) Transwell migration assay of A7r5 cells. (*E–F*) Quantitative analysis of scratch assay and transwell migration assay. Each experiment was repeated a minimum of 3 times. One-way ANOVA; mean ± standard deviation; $^{\#,*,+}P < .05$; $^{\#\#,**,++}P < .01$.

and increasing SVR and SMA resistance. Therefore, metformin may not entirely depend on the amelioration of liver cirrhosis to alleviate the splanchnic hemodynamic alterations in BDL rats, which provides significant clues for us to further elucidate the underlying mechanism by which metformin improves PHT in cirrhosis.

Arterial remodeling in cirrhotic rats is supported by previous studies, which reported a remarkable decrease in

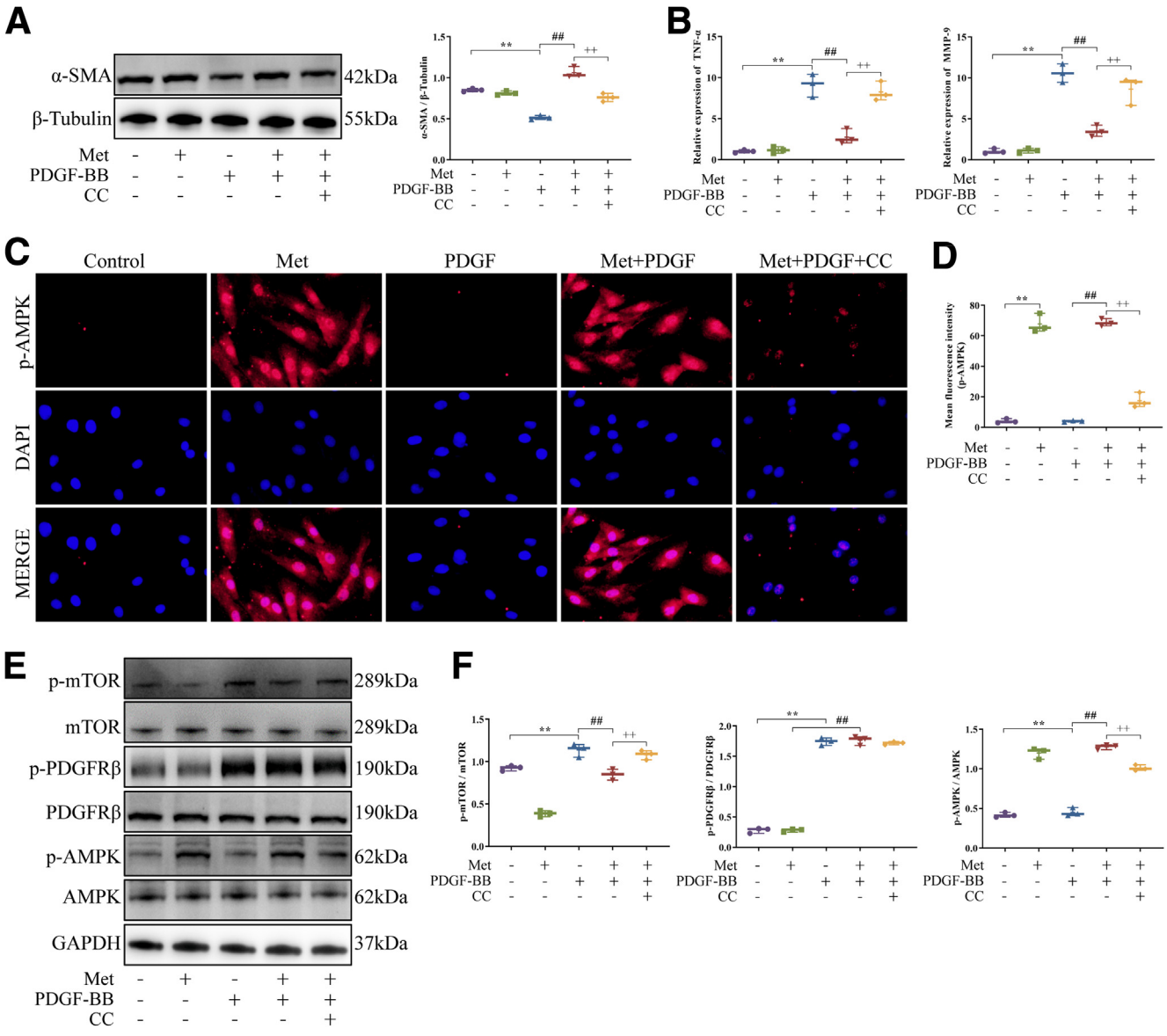

Figure 8. Metformin activates AMPK to inhibit PDGF-BB-induced phenotypic switch in A7r5 cells. (*A*) The expression level of α-SMA contractile protein in A7r5 cells. (*B*) The relative expression levels of TNF-α and MMP9 in A7r5 cells. (*C*) Immunofluorescence staining of p-AMPK expression in A7r5 cells. (*D*) Quantitative analysis of p-AMPK expression. (*E–F*) The expression levels of p-mTOR, p-PDGFRβ, and p-AMPK in A7r5 cells. Each experiment was repeated a minimum of 3 times. One-way ANOVA; mean ± standard deviation; $^{\#,*,+}P < .05$; $^{\#\#,**,++}P < .01$.

the vascular wall thickness and a reduction in the wall thickness/lumen diameter ratio, serving as an indicator of vascular contractility.[6] The results of the current study indicated that metformin exhibited a beneficial effect on SMA wall thickness in BDL rats, notably increased the thickness of the arterial smooth muscle layer, thus ameliorating arterial remodeling. In mature animal vessels, VSMCs display a contractile phenotype characterized by the expression of various contractile proteins, such as α-SMA, SM22α, and smooth muscle myosin heavy chain (SM-MHC).[28,29] These contractile VSMCs organize circumferentially to form the arterial medial layer, contributing to contractility, structural integrity, and vascular elasticity.[30] Following 4 and 6 weeks post-BDL, there was a remarkable downregulation in the expression levels of α-SMA and SM22α in the SMA. However, our findings demonstrated that metformin enhanced the expression of contractile proteins α-SMA and SM22α in the SMA of BDL rats. It was tempting to speculate that metformin may potentially inhibit the dedifferentiation of contractile VSMCs in the SMA of BDL rats by enhancing the expression of contractile proteins, thereby alleviating arterial remodeling. Furthermore, as demonstrated by Gunarathne et al, the blockade of the renin angiotensin system (RAS) receptors improved the hyperdynamic circulatory state in cirrhosis, indicating that splanchnic arteries remained responsive to drugs despite

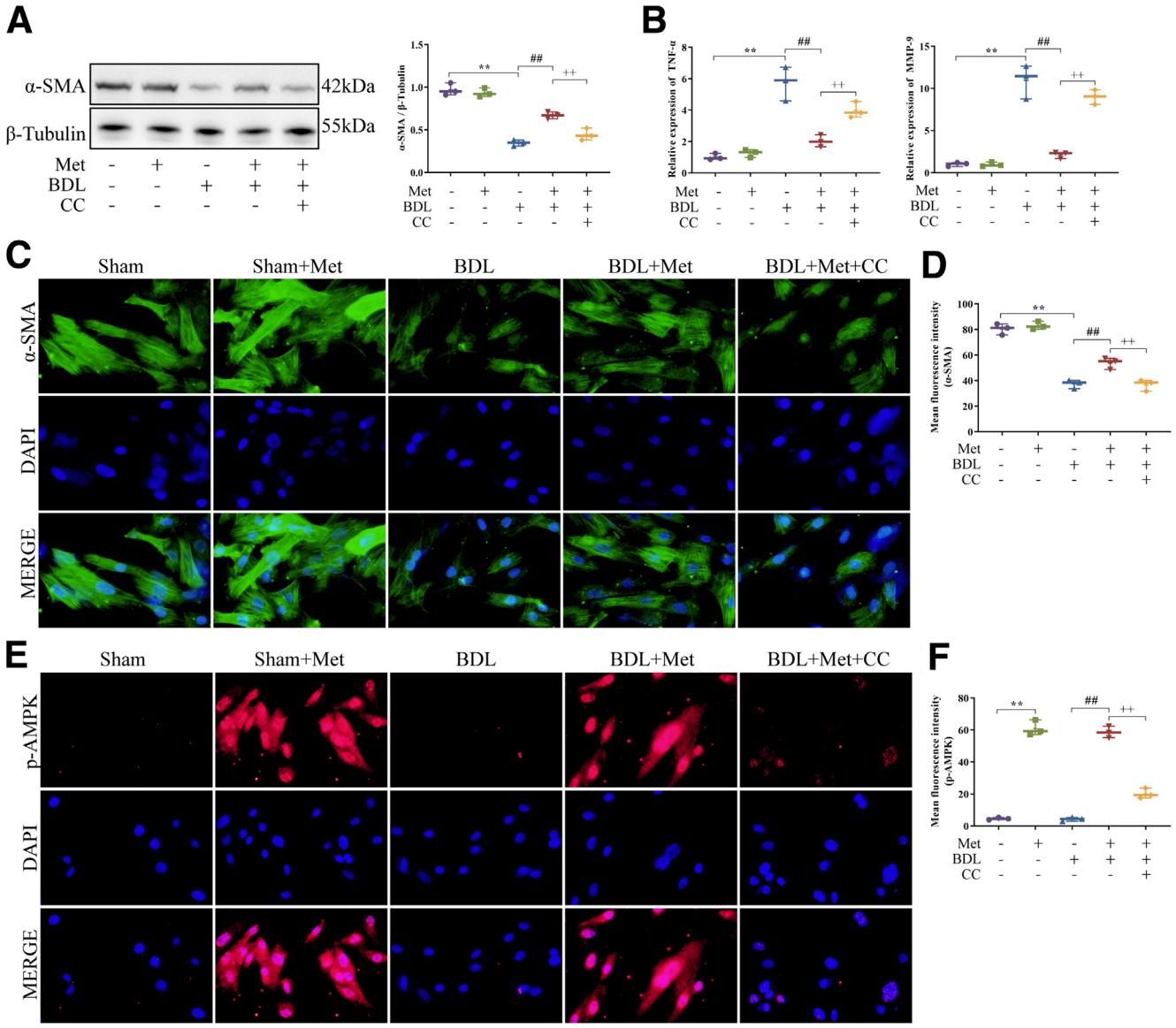

Figure 9. Metformin activates AMPK to increase the contractile proteins in primary VSMCs from BDL rats. (*A*) The expression level of α-SMA contractile protein in primary VSMCs. (*B*) The relative expression levels of TNF-α and MMP9 in primary VSMCs. (*C*) IF staining of α-SMA expression in primary VSMCs. (*D*) Quantitative analysis of α-SMA expression. (*E*) IF staining of p-AMPK expression in primary VSMCs. (*F*) Quantitative analysis of p-AMPK expression. Each experiment was repeated a minimum of 3 times. One-way ANOVA; mean ± standard deviation; $^{\#,\star,+}P < .05$; $^{\#\#,\star\star,++}P < .01$.

the presence of arterial remodeling in cirrhosis.[31] Therefore, following the improvement of arterial remodeling by metformin, the effect of blocking the RAS receptors on ameliorating the splanchnic hyperdynamic circulation in cirrhosis might be enhanced.

Vascular disorders are correlated with the phenotypic switching of VSMCs. Interestingly, this phenotypic switching of VSMCs is recognized as a critical factor in the pathogenesis of aneurysm formation.[20,32] Under pathologic conditions such as vascular injury, shear stress forces, and growth factor stimulation, downregulation of VSMCs contractile markers and upregulation of synthetic markers indicate the transition of VSMCs from a contractile to a synthetic phenotype. Similarly, the phenotypic switching of VSMCs led to arterial remodeling in the splanchnic vascular of cirrhotic rats with PHT, as revealed in our previous studies.[8] Chronic inflammation resulting from liver cirrhosis, increased vascular shear stress due to PHT and hyperdynamic circulation, along with the upregulation of vascular growth factors such as PDGF-BB, may collectively drive the differentiation of contractile VSMCs, thereby contributing to arterial remodeling in cirrhotic rats. Our findings confirmed a marked increase in the expression of synthetic VSMCs markers in BDL rats, including IL-1β, IL-6, TNF-α, and MMP9. Conversely, there is a notable decrease in the expression of contractile VSMCs markers, including

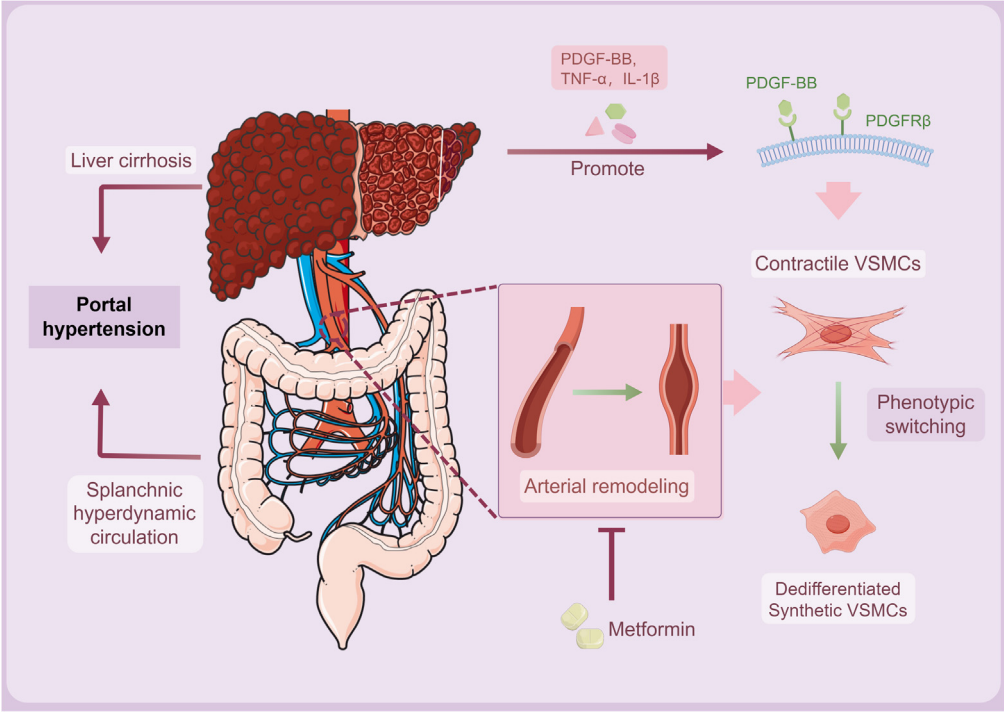

Figure 10. A schematic illustrating how metformin modulates VSMCs phenotype switching to improve PHT in cirrhotic rats. Metformin inhibits the phenotype switching of VSMCs induced by PDGF-BB from a contractile to a synthetic phenotype, resulting in the upregulation of VSMC-specific contractile markers α-SMA and SM22α, thereby mitigating arterial remodeling and hyperdynamic splanchnic circulation in cirrhotic rats. (Diagram was generated by Figdraw and SMART servier).

contractile proteins α-SMA and SM22α. Furthermore, metformin had shown the capacity to suppress the dedifferentiation of contractile VSMCs, by downregulating the expression of inflammatory factors and upregulating contractile proteins, leading to improvements in arterial dilation and remodeling in both the early and advanced stages of cirrhosis. Consequently, the present study offers a novel perspective on exploring the regulatory mechanism underlying the splanchnic hyperdynamic circulation in cirrhosis with PHT.

PDGF-BB is known as one of the most potent factors driving phenotypic switching in VSMCs, from a differentiated to a dedifferentiated phenotype.[33] It is noteworthy that the excessive enhancement of PDGF-BB/PDGFR-β signaling represents a critical feature in the progress of liver fibrosis.[14] Interestingly and importantly, our transcriptome sequencing analysis revealed a significant upregulation in the expression of PDGFRβ within the mesenteric arteries of BDL rats. As expected, our current findings confirmed a significant increase in PDGF-BB expression in BDL rats. Moreover, metformin markedly reduced the expression levels of PDGF-BB and downregulated PDGFRβ phosphorylation in SMA of BDL rats, thereby inhibiting activation of the PDGFRβ signaling pathway. Furthermore, previous evidence indicated that PDGF-BB affected various signaling pathways in VSMCs, including the PI3K/AKT/mTOR pathway.[34] Notably, mTOR served as a downstream target of these pathways, playing a crucial role in VSMCs phenotypic modulation. For example, rapamycin inhibited the activation of the mTOR pathway, resulting in the suppression of VSMC proliferation and improvement in pulmonary vascular remodeling.[35] Similarly, studies have shown that chicoric acid hindered PDGF-BB-induced VSMC phenotypic switching, proliferation, and migration by inhibiting the mTOR/P70S6K signaling cascade.[36] In addition, it is widely acknowledged that AMPK acts as a negative regulator of the mTOR pathway. Recent findings have shown that the activation of AMPK inhibited PDGF-BB-induced VSMC dedifferentiation by suppressing the mTOR signaling pathway.[37,38] In the present study, we demonstrated that metformin induced an upregulation in the expression of p-AMPK and p-ACC, resulting in the activation of the AMPK signaling cascade. This activation significantly attenuated mTOR phosphorylation and disrupted the downstream signaling induced by PDGF-BB/PDGFRβ, consequently suppressing the dedifferentiation of contractile VSMCs and ameliorating arterial remodeling in cirrhotic rats.

The phenotypic switching of VSMCs is extremely complicated and exhibits greater heterogeneity in various vascular diseases. Despite observing the beneficial effects of metformin in BDL rats, it is crucial to acknowledge the inherent complexity and dynamism of *in vivo* studies. The results of our *in vitro* experiments showed that PDGF-BB induced phenotypic switching in A7r5 cells, promoting cell proliferation and migration, along with downregulation of contractile proteins and upregulation of TNF-α and MMP9 expression. Notably, primary VSMCs isolated from BDL rats exhibited similar phenotypic features. Upon activation of PDGFRβ by PDGF-BB, mTOR signaling pathways were subsequently activated. However, metformin suppressed the dedifferentiation of VSMCs by activating AMPK and subsequently inhibiting the downstream mTOR pathway. Our findings were consistent with the previous study that AMPK activation favored the switch of the synthetic phenotype of VSMCs toward a contractile phenotype.[39] Moreover, treatment with AMPK inhibitor Compound C reversed these

beneficial effects of metformin in both A7r5 cells and primary VSMCs cells. Collectively, our study demonstrated the potential mechanism of metformin in effectively suppressing PDGF-BB-induced phenotypic switching of VSMCs through the activation of AMPK signaling pathway. Contractile VSMCs play a crucial role in stabilizing vascular structures, thereby alleviating arterial vasodilation and remodeling. These findings provide a novel insight into the role and underlying mechanisms of VSMCs in the process of splanchnic arterial remodeling associated with liver cirrhosis.

Conclusion

In summary, our study demonstrated the effects of metformin on ameliorating PHT and splanchnic hyperdynamic circulation in cirrhotic rats, even in advanced stages. Our findings revealed that metformin improved arterial remodeling in BDL rats by inhibiting the dedifferentiation of contractile VSMCs through activating AMPK to block the downstream pathway of PDGFRβ. We proposed for the first time to elucidate the potential mechanism underlying arterial remodeling in liver cirrhosis from the VSMCs perspective. These novel insights may facilitate the development of innovative therapeutic approaches targeting PHT and its associated life-threatening vascular complications in advanced liver cirrhosis.

Materials and methods

Animal Models

Male Sprague Dawley (SD) rats, weighing 200 to 250 g and aged 6 to 8 weeks, were obtained from the Experimental Animal Center of Shanghai Jiao Tong University School of Medicine. The rats were housed in specific pathogen-free facilities with a humidity of 40% to 60%, temperature maintained at 24 °C, and a 12-hour light/dark cycle, with ad libitum access to food and water. As previously described,[8] all SD rats underwent either sham surgery (Sham) or common BDL. The experimental protocol involving rats was approved by the Ethics Committee of Shanghai Ninth People's Hospital, Shanghai Jiao Tong University School of Medicine.

In the long-term early metformin treatment group, the metformin or vehicle (distilled water) was administered starting immediately on the first day following BDL surgery and was continued for 4 weeks. On the 29th day post-BDL, rats were euthanized and subjected to relevant experiments (n = 6 per group). Conversely, in the long-term late metformin treatment group, the metformin or vehicle was initiated on the 15th day post-BDL, by which time significant liver fibrosis had already occurred, gradually progressing into the irreversible late stages of cirrhosis. On the 43rd day after operations, the experiments were performed (n = 6 per group).

Hemodynamic Measurements

Based on our previous study,[8] rats were anesthetized by inhalation of isoflurane (1.5%–2%), and PE50 catheters were carefully inserted into the portal vein or femoral artery. These PE50 catheters were then connected to pressure transducers to detect the values of PP, heart rate (HR), and mean arterial pressure (MAP) using an ALC-MPA multichannel biological information analysis system (Shanghai Alcott Biotech Co).

Echocardiographic data was acquired using a transthoracic echocardiogram.[40] After anesthesia in an induction chamber, SD rats were placed in the supine position. Hair was removed from the chest using a depilatory cream, followed by a water rinse, to facilitate echocardiographic data collection. Subsequently, the SMA of the rats was identified from its origin at the aorta, and SMA blood flow was measured using a pulsed Doppler flow transducer.[41] The ultrasonography system (Vevo 2100 system, Fujifilm Visual Sonics) was used to measure the SMA flow of rats. The SMA flow was measured at the proximal 1- to 2-cm segment of the SMA near to its origin from the aorta. Angle of insonation should be maintained as low as possible to minimize the errors in calculations of velocity.[42] The mean of the 3 luminal diameter (mm) and 3 blood flow velocity (mm/s) were obtained at each scan to increase reproducibility.[43,44] The SMA flow rate was then calculated using the formula: SMA flow rate = luminal cross sectional area × blood flow velocity.

The stroke volume (SV) of the rat heart was obtained by dividing the CO by the HR (mL/beat). The CI (mL/min/100 g) was determined as the CO per 100 g of body weight. SVR (mmHg/mL/min/100 g) was calculated by dividing the MAP by the CI. SMA resistance (mmHg/mL/min/100 g) was calculated as (MAP-PP)/SMA flow per 100 g.

Blood Biochemistry Analysis and Enzyme-linked Immunosorbent Assay

Peripheral blood was collected from SD rats, and serum was obtained after centrifugation at 3000 RPM for 20 minutes. Subsequently, the serum samples were analyzed for ALT, AST, and TBIL levels. This analysis was performed using an automated clinical analyzer (Hitachi Ltd).

The serologic assays were performed using enzyme-linked immunosorbent assay (ELISA). Levels of TNF-α, IL-1, IL-6, VEGFA, and PDGF-BB in rat serum were measured using ELISA kits (ELK1396, ELK1272, ELK1158, ELK2320, ELK9486, ELK Biotechnology) according to the instructions of the manufacturer.

Histologic and Immunohistochemistry/ Immunofluorescence Analysis

The right hepatic lobe and mesenteric tissue of rats were immersed in 10% formalin buffer (pH 7.4) for fixation and subsequently embedded in paraffin blocks. Following this, liver and mesenteric tissue sections underwent staining with H&E, Masson's trichrome, and Sirius red. Thereafter, an experienced pathologist conducted random examination of all tissue sections utilizing an optical microscope.

Immunohistochemistry (IHC) and IF analyses were performed on paraffin-embedded liver and mesenteric tissue sections. Cells were seeded and fixed using 4% paraformaldehyde following the IF protocol. To inhibit

endogenous peroxidase activity, a solution of methanol containing 0.3% H_2O_2 was applied. Antigen retrieval was achieved using citrate buffer. To prevent nonspecific binding of antibodies, incubation with 10% normal horse serum was carried out. The sections were then incubated overnight at 4 °C to the primary antibodies listed as follows: anti-CD31 antibody (1:200, ab222783, Abcam), anti-CD68 antibody (1:200, ab283654, Abcam), anti-α-SMA antibody (1:200, ab5694, Abcam), anti-SM22α antibody (1:200, ab213273, Abcam), and anti-phospho-AMPK antibody (1:150, ab23875, Abcam). Phosphate-buffered saline (PBS) served as the negative control. Subsequently, the sections were incubated with secondary antibodies at room temperature for 60 minutes. Slides were then treated with hematoxylin, dehydrated, and mounted for IHC, or mounted with Slowfade Mountant + DAPI and sealed for IF. The sections were visualized and captured using a fluorescence microscope.

RNA Preparation and RT-qPCR

Total RNA was extracted from VSMCs or mesenteric arteries using TRIzol reagent (Invitrogen) following the manufacturer's instructions. Subsequently, cDNA synthesis was performed using the PrimeScriptTM RT reagent kit (TAKARA). PCR amplification was carried out on the ABI 7900HT Real-Time PCR system using the SYBR Green PCR Mastermix Kit (Yeasen). The internal control was used by glyceraldehyde 3-phosphate dehydrogenase (GAPDH), and all experiments were conducted in triplicate. The relative mRNA expression was determined using the $2^{-\Delta\Delta Ct}$ method.

Western Blotting Analysis

Liver and mesenteric arteries obtained from rats were promptly stored at −80 °C until further analysis. To extract protein from these tissues or cells, the samples were homogenized with RIPA buffer (Beyotime) according to the manufacturer's instructions. Subsequently, the resulting tissue or cells extracts underwent centrifugation at 12,000 × RPM for 15 minutes at 4 °C. The supernatant obtained after centrifugation was meticulously collected, and the total protein concentration was determined using a BCA protein analysis kit (Beyotime). Equivalent quantities of proteins were loaded onto sodium dodecyl sulfate-polyacrylamide gel electrophoresis (SDS-PAGE) and subsequently transferred onto PVDF membranes through electrotransfer. Immunoblotting was performed using primary antibodies targeting p-PDGFRβ (ABclonal), PDGFRβ (ABclonal), endothelial nitric oxide synthase (eNOS) (Cell Signaling), p-eNOS (Cell Signaling), vascular endothelial growth factor receptor 2 (VEGFR2, ABclonal), p-VEGFR2 (ABclonal), α-SMA (Abcam), SM22α (Abcam), p-AMPK (Abcam), AMPK (Abcam), acetyl-CoA carboxylase (ACC) (Cell Signaling), p-ACC (Cell Signaling), mammalian target of rapamycin (mTOR) (Cell Signaling), p-mTOR (Cell Signaling), β-Tubulin (Proteintech), and GAPDH (Proteintech). Following antibody incubation, the membranes were treated with secondary antibodies for 1 hour at 24 °C and visualized using an enhanced chemiluminescence detection kit (Millipore Corporation).

Primary VSMCs Isolation and Culture

VSMCs were isolated from the SMAs of SD rats using an explant technique, as previously described.[45] Subsequently, these cells were cultured in Dulbecco's modified Eagle's medium (DMEM) (Hyclone) supplemented with 10% fetal bovine serum (FBS) (Gibco), and 1% antibiotics at 37 °C with 5% CO_2. VSMCs were identified through positive labeling with anti-α-SMA antibody and examination of cell morphology. Only cells within passages 3 to 8 were utilized in the present study.

Cell Viability and Proliferation Assay

The cytotoxicity of metformin was evaluated using the Cell Counting Kit-8 (CCK8, Dojindo) assay as the manufacturer's instructions. Briefly, VSMCs were seeded at a density of 8×10^3 cells/well in a 96-well plate with 100 μL complete culture medium. After treatment with varying concentrations of metformin for 48 hours, cell viability was measured by adding 90 μL incomplete culture medium and 10 μL CCK-8 reagent to each well, followed by incubation at 37 °C for 2 hours. The absorbance was measured at 450 nm.

Cell proliferation was assessed using the CCK8 assay. VSMCs were seeded in 96-well plates at a density of 5×10^3 cells/well. At 0, 24, 48, 72, and 96 hours, the cells were incubated with the CCK8 reagent and incomplete culture medium for 2 hours at 37 °C and 5% CO_2. A growth curve was generated by measuring the absorbance at 450 nm every 24 hours for 5 consecutive days using a spectrophotometer (Thermo).

Cell Migration Assay

Scratch healing assay was employed to assess the migration ability of VSMCs. VSMCs were cultured in small dishes to sub-fusion, followed by incubation with FBS-free medium. Linear scratches were created using sterile plastic microtube heads. Images were acquired at the outset and at regular intervals during the migration process to monitor wound closure. The percentage of cell healing = (scratch width before experiment − scratch width after experiment) / scratch width before experiment × 100%.

Transwell permeable supports (24-well, 3.0-μm membrane; Corning) were utilized to evaluate cell migration. VSMCs were seeded at a concentration of 5×10^4 cells/mL in the upper chamber with FBS-free medium, whereas DMEM containing 10% FBS was added to the lower chamber. After incubation for 24 hours, cells that had migrated from the upper chamber were fixed using 4% paraformaldehyde, stained with crystal violet solution, and subsequently counted under a light microscope.

Statistical Analysis

The data in this study were presented as mean ± standard deviation (SD). Statistical analysis was performed using 1-way analysis of variance (ANOVA) followed by a post-hoc Student t-test. A $P < .05$ was considered statistically significant. The data was analyzed and graphed using SPSS (version 23.0) and GraphPad Prism (version 7.0) software.

References

1. Gines P, Krag A, Abraldes JG, et al. Liver cirrhosis. Lancet 2021;398:1359–1376.
2. Nelms DW, Pelaez CA. The acute upper gastrointestinal bleed. Surg Clin North Am 2018;98:1047–1057.
3. Alqahtani SA, Jang S. Pathophysiology and management of variceal bleeding. Drugs 2021;81:647–667.
4. Thalheimer U, Triantos CK, Samonakis DN, et al. Infection, coagulation, and variceal bleeding in cirrhosis. Gut 2005;54:556–563.
5. Fernandez-Varo G, Morales-Ruiz M, Ros J, et al. Impaired extracellular matrix degradation in aortic vessels of cirrhotic rats. J Hepatol 2007;46:440–446.
6. Fernandez-Varo G, Ros J, Morales-Ruiz M, et al. Nitric oxide synthase 3-dependent vascular remodeling and circulatory dysfunction in cirrhosis. Am J Pathol 2003; 162:1985–1993.
7. Iwakiri Y, Shah V, Rockey DC. Vascular pathobiology in chronic liver disease and cirrhosis - current status and future directions. J Hepatol 2014;61:912–924.
8. Wu G, Chen M, Fan Q, et al. Transcriptome analysis of mesenteric arterioles changes and its mechanisms in cirrhotic rats with portal hypertension. BMC Genomics 2023;24:20.
9. Paredes F, Williams HC, Quintana RA, San Martin A. Mitochondrial protein Poldip2 (Polymerase Delta Interacting Protein 2) controls vascular smooth muscle differentiated phenotype by O-linked GlcNAc (N-Acetylglucosamine) transferase-dependent inhibition of a ubiquitin proteasome system. Circ Res 2020;126:41–56.
10. Sansbury BE, Spite M. Resolution of acute inflammation and the role of resolvins in immunity, thrombosis, and vascular biology. Circ Res 2016;119:113–130.
11. Wortmann M, Arshad M, Hakimi M, et al. Deficiency in Aim2 affects viability and calcification of vascular smooth muscle cells from murine aortas and angiotensin-II induced aortic aneurysms. Mol Med 2020;26:87.
12. Chen W, Liu DJ, Huo YM, et al. Reactive oxygen species are involved in regulating hypocontractility of mesenteric artery to norepinephrine in cirrhotic rats with portal hypertension. Int J Biol Sci 2014;10:386–395.
13. Neaud V, Rosenbaum J. A red wine polyphenolic extract reduces the activation phenotype of cultured human liver myofibroblasts. World J Gastroenterol 2008;14:2194–2199.
14. Wang X, Wu X, Zhang A, et al. Targeting the PDGF-B/PDGFR-beta interface with destruxin A5 to selectively block PDGF-BB/PDGFR-betabeta signaling and attenuate liver fibrosis. EBioMedicine 2016;7:146–156.
15. Kang H, Ahn DH, Pak JH, et al. Magnobovatol inhibits smooth muscle cell migration by suppressing PDGF-Rbeta phosphorylation and inhibiting matrix metalloproteinase-2 expression. Int J Mol Med 2016; 37:1239–1246.
16. Castera L, Cusi K. Diabetes and cirrhosis: current concepts on diagnosis and management. Hepatology 2023; 77:2128–2146.
17. Zhang A, Qian F, Li Y, et al. Research progress of metformin in the treatment of liver fibrosis. Int Immunopharmacol 2023;116:109738.
18. Li Z, Ding Q, Ling LP, et al. Metformin attenuates motility, contraction, and fibrogenic response of hepatic stellate cells in vivo and in vitro by activating AMP-activated protein kinase. World J Gastroenterol 2018;24:819–832.
19. Adachi M, Brenner DA. High molecular weight adiponectin inhibits proliferation of hepatic stellate cells via activation of adenosine monophosphate-activated protein kinase. Hepatology 2008;47:677–685.
20. Li S, Shi Y, Liu P, et al. Metformin inhibits intracranial aneurysm formation and progression by regulating vascular smooth muscle cell phenotype switching via the AMPK/ACC pathway. J Neuroinflammation 2020;17:191.
21. Lee MH, Kwon BJ, Seo HJ, et al. Resveratrol inhibits phenotype modulation by platelet derived growth factor-bb in rat aortic smooth muscle cells. Oxid Med Cell Longev 2014;2014:572430.
22. Zhang X, Feng T, Zeng XI, et al. Identification of transcriptional variation in aortic remodeling using a murine transverse aortic constriction (TAC) model. Front Cardiovasc Med 2020;7:581362.
23. Iwakiri Y. Pathophysiology of portal hypertension. Clin Liver Dis 2014;18:281–291.
24. Iwakiri Y, Groszmann RJ. The hyperdynamic circulation of chronic liver diseases: from the patient to the molecule. Hepatology 2006;43(2 Suppl 1):S121–S131.
25. Orr AW, Hastings NE, Blackman BR, Wamhoff BR. Complex regulation and function of the inflammatory smooth muscle cell phenotype in atherosclerosis. J Vasc Res 2010;47:168–180.
26. Gunthel M, Barnett P, Christoffels VM. Development, proliferation, and growth of the mammalian heart. Mol Ther 2018;26:1599–1609.
27. Fan Q, Wu G, Chen M, et al. Cediranib ameliorates portal hypertensive syndrome via inhibition of VEGFR-2 signaling in cirrhotic rats. Eur J Pharmacol 2024;964: 176278.
28. Huang C, Huang W, Wang R, He Y. Ulinastatin inhibits the proliferation, invasion and phenotypic switching of PDGF-BB-induced VSMCs via Akt/eNOS/NO/cGMP signaling pathway. Drug Des Devel Ther 2020; 14:5505–5514.
29. Lu L, Sun X, Chen C, et al. Shexiang baoxin pill, derived from the traditional Chinese medicine, provides protective roles against cardiovascular diseases. Front Pharmacol 2018;9:1161.
30. Hu D, Yin C, Luo S, et al. Vascular smooth muscle cells contribute to atherosclerosis immunity. Front Immunol 2019;10:1101.
31. Gunarathne LS, Rajapaksha IG, Casey S, et al. Mas-related G protein-coupled receptor type D antagonism improves portal hypertension in cirrhotic rats. Hepatol Commun 2022;6:2523–2537.
32. Salmon M, Johnston WF, Woo A, et al. KLF4 regulates abdominal aortic aneurysm morphology and deletion attenuates aneurysm formation. Circulation 2013;128(11 Suppl 1):S163–S174.
33. Holycross BJ, Blank RS, Thompson MM, et al. Platelet-derived growth factor-BB-induced suppression of smooth muscle cell differentiation. Circ Res 1992; 71:1525–1532.

34. Chen Z, Wu Q, Yan C, Du J. COL6A1 knockdown suppresses cell proliferation and migration in human aortic vascular smooth muscle cells. Exp Ther Med 2019; 18:1977–1984.
35. Pena A, Kobir A, Goncharov D, et al. Pharmacological inhibition of mTOR kinase reverses right ventricle remodeling and improves right ventricle structure and function in rats. Am J Respir Cell Mol Biol 2017; 57:615–625.
36. Lu QB, Wan MY, Wang PY, et al. Chicoric acid prevents PDGF-BB-induced VSMC dedifferentiation, proliferation and migration by suppressing ROS/NFkappaB/mTOR/P70S6K signaling cascade. Redox Biol 2018; 14:656–668.
37. Hwang YJ, Park JH, Cho DH. Activation of AMPK by telmisartan decreases basal and PDGF-stimulated VSMC proliferation via inhibiting the mTOR/p70S6K signaling axis. J Korean Med Sci 2020;35:e289.
38. Hwang YJ, Park JH, Cho DH. Far-infrared irradiation decreases proliferation in basal and PDGF-stimulated VSMCs through AMPK-mediated inhibition of mTOR/p70S6K signaling axis. J Korean Med Sci 2023;38:e335.
39. Garcia-Prieto CF, Gil-Ortega M, Vega-Martin E, et al. Beneficial effect of bariatric surgery on abnormal MMP-9 and AMPK activities: potential markers of obesity-related CV risk. Front Physiol 2019;10:553.
40. Slama M, Susic D, Varagic J, et al. Echocardiographic measurement of cardiac output in rats. Am J Physiol Heart Circ Physiol 2003;284:H691–H697.
41. Hsu SJ, Lee FY, Wang SS, et al. Caffeine ameliorates hemodynamic derangements and portosystemic collaterals in cirrhotic rats. Hepatology 2015;61:1672–1684.
42. Gatt M, MacFie J, Anderson AD, et al. Changes in superior mesenteric artery blood flow after oral, enteral, and parenteral feeding in humans. Crit Care Med 2009; 37:171–176.
43. Wu J, Agbor LN, Fang S, et al. Failure to vasodilate in response to salt loading blunts renal blood flow and causes salt-sensitive hypertension. Cardiovasc Res 2021;117:308–319.
44. Geelkerken RH, Lamers CB, Delahunt TA, et al. Duodenal meal stimulation leads to coeliac artery vasoconstriction and superior mesenteric artery vasodilatation: an intra-abdominal ultrasound study. Ultrasound Med Biol 1998;24:1351–1356.
45. Duan C, Wang L, Zhang J, et al. Mdivi-1 attenuates oxidative stress and exerts vascular protection in ischemic/hypoxic injury by a mechanism independent of Drp1 GTPase activity. Redox Biol 2020;37:101706.

Received August 13, 2024. Accepted February 24, 2025.

Correspondence
Address correspondence to: Dr Meng Luo, Dr Haizhong Huo, and Dr Lei Zheng, Department of General Surgery, Shanghai Ninth People's Hospital Affiliated to Shanghai Jiao Tong University School of Medicine, Shanghai 200011, China. e-mail: hzhhuodr7@sina.com; zl1055174020@163.com; luosh9hospital@sina.com.

CRediT Authorship Contribution

Guangbo Wu (Conceptualization: Lead; Data curation: Lead; Formal analysis: Lead; Methodology: Lead; Project administration: Lead; Software: Lead; Writing – original draft: Lead)

Qiang Fan (Conceptualization: Equal; Data curation: Equal; Methodology: Lead)

Min Chen (Formal analysis: Equal; Methodology: Equal; Writing – review & editing: Equal)

Guqing Luo (Methodology: Lead; Software: Equal)

Zhenghao Wu (Data curation: Equal; Software: Lead)

Jinbo Zhao (Methodology: Equal; Validation: Equal)

Jiayun Lin (Formal analysis: Equal; Methodology: Equal; Resources: Supporting)

Chihao Zhang (Formal analysis: Lead; Resources: Supporting; Software: Equal)

Hongjie Li (Investigation: Supporting; Methodology: Supporting)

Xiaoliang Qi (Project administration: Supporting; Supervision: Supporting)

Haizhong Huo (Funding acquisition: Supporting; Supervision: Supporting)

Lei Zheng (Funding acquisition: Lead; Methodology: Equal; Resources: Equal)

Meng Luo (Conceptualization: Lead; Data curation: Equal; Formal analysis: Equal; Funding acquisition: Lead; Project administration: Lead; Writing – review & editing: Lead)

Conflicts of interest
The authors disclose no conflicts.

Funding
This study was supported by the National Natural Science Foundation of China (82100639, 82200630, 81970526), the Fundamental research program funding of Ninth People's Hospital affiliated to Shanghai Jiao Tong University School of Medicine (JYZZ162), the Clinical Research Program of 9th People's Hospital, Shanghai Jiao Tong University School of Medicine (JYLJ202124), and the 'Unveiling and Leadership' Series Project of Renji Hospital Discipline Development Pinnacle Plan (RJTJ25-QN-030).

Data Availability
The sequencing data (RNA-seq) generated and analyzed in the current study are available in the Sequence Read Archive (SRA) of the National Center for Biotechnology Information (NCBI) under the BioProject accession number of PRJNA859251.